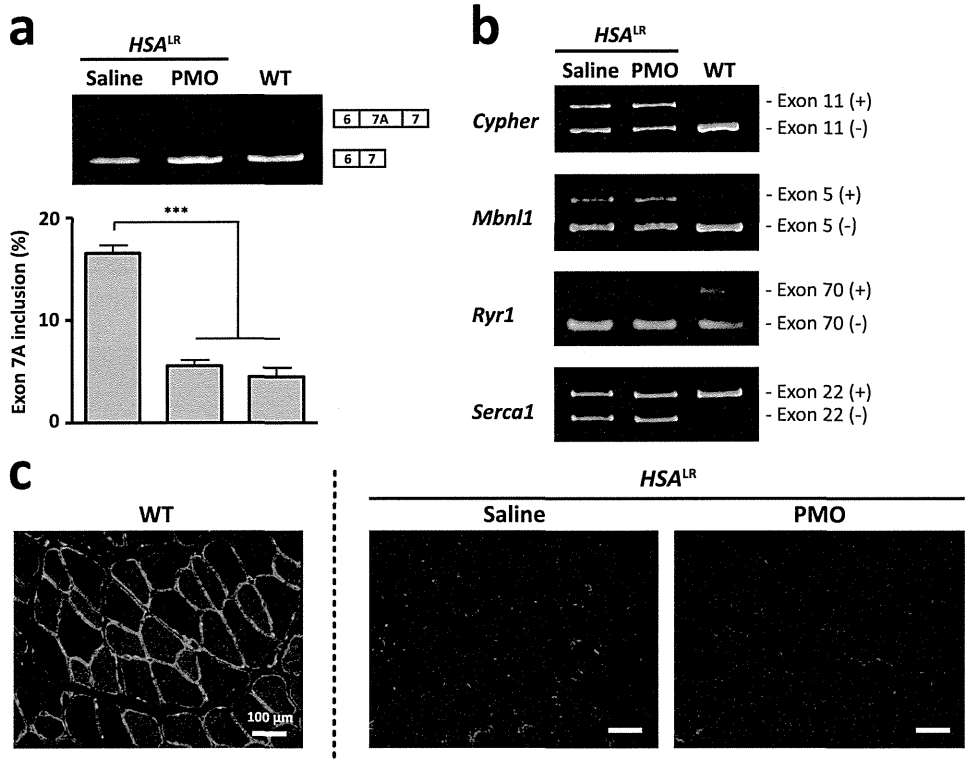

Figure 3 | *In vivo* improvement of aberrant splicing of the *Clcn1* gene by 1–25 PMO. (a) The alternative splicing of *Clcn1* exon 7A in HSA^{LR} and WT mice. 1–25 PMO (20 μg) or saline was locally administrated into TA muscles of HSA^{LR} mice. The ratio of the splicing variant containing exon 7A in thevPMO-injected muscles decreased to a level comparable with that in WT muscle ($n = 5$). The bars indicate mean and s.e.m., and statistical significance was analysed by Tukey's multi-comparison test (*** $P < 0.001$). (b) Abnormal splicing of other genes in HSA^{LR} mice was not affected by 1–25 PMO. (c) Immunofluorescence analysis of transverse sections of TA muscle with an anti-Clcn1 antibody. Injection of 1–25 PMO restored the sarcolemmal localisation of Clcn1 protein in TA muscles of HSA^{LR} mice.

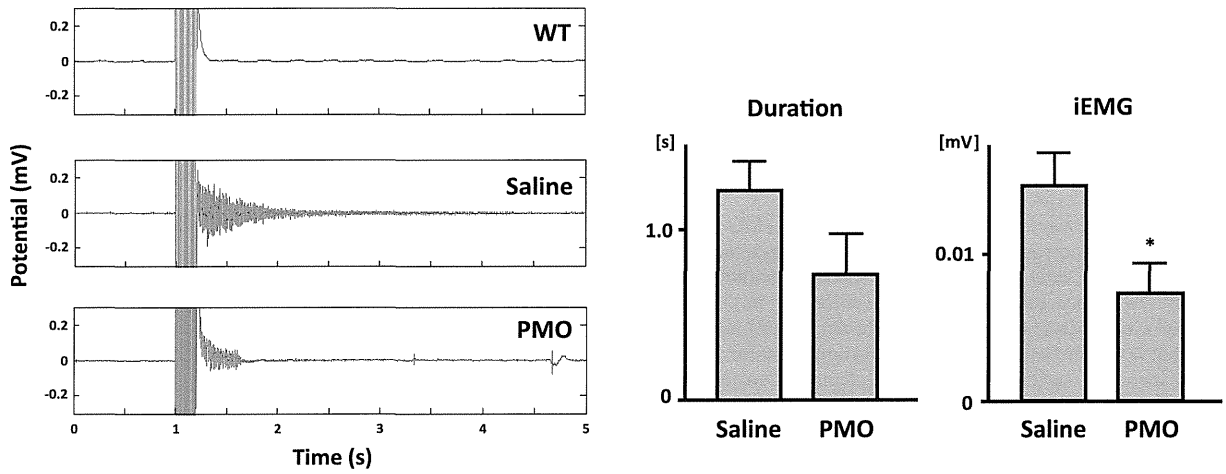

Figure 4 | Reduction of myotonic discharge by 1–25 PMO in HSA^{LR} mice. (a) Representative EMG signals of TA muscle. Tibialis muscle was electrically stimulated 1 s after the EMG recording started. In the HSA^{LR} muscle, repetitive discharges that were absent in the WT muscle could be seen. (b)vDuration of myotonic discharge and integrated EMG (iEMG). 1–25 PMO significantly reduced iEMG in HSA^{LR} muscle (saline, $n = 6$; 1–25 PMO, $n = 7$).The bars indicate mean and s.d., and statistical significance was analysed by Student's *t*-test (* $P < 0.05$).

phenotypic levels, and that the Bubble liposome-ultrasound system should be capable of delivering enough PMO to ameliorate myotonia.

Discussion

The greatest advantage of PMO is its remarkable innocuity. According to a report from Gene Tools, administration of a single 700 mg/kg dose of PMO to a mouse did not cause any obvious acute toxicity[31], while the 50% lethal dose of phosphorothioate DNA, a first-generation antisense oligonucleotide, was estimated to be 750 mg/kg in mice[32]. The high pharmaceutical potential of PMO is also supported by the fact that safety issues were not raised following its administration to mice and humans; however, PMO must overcome the low permeability of the cell membranes to achieve a significant effect on alternative splicing. Because of the inefficient cellular uptake of PMO, systemic delivery and functional splicing modification were not successful in a mouse model[33]. Therefore, for the clinical application of PMO, establishing an effective delivery method is essential.

The major achievement in this study was that we increased the efficiency of PMO delivery using Bubble liposomes and ultrasound. The use of the ultrasound-mediated delivery system with Bubble liposomes improved the alternative splicing of the *Clcn1* gene in HSA^{LR} mice to a level comparable to that of wild-type mice and decreased myotonic discharges, indicating that the delivery system increased introduction of 1–25 PMO into skeletal muscle. Our results show that the intramuscular injection itself delivered the PMO into muscle to some extent, and so the intramuscular injection might have contributed to the relief of the pathology. However, the Bubble liposome- and ultrasound-mediated enhancement of delivery efficiency suggests that the new delivery system will have a beneficial effect over much less invasive injection, such as intravenous injection, which cannot by itself be expected to promote the entry of PMO into skeletal muscle[19].

A fair amount of the *Clcn1* splicing variant without exon 7A was expressed even in the HSA^{LR} mouse. Because the myotonic discharge of a HSA^{LR} mouse was remedied by correcting *Clcn1* alternative splicing in a previous study[14], abnormal splicing of the gene must be the primary cause of myotonia. The expression levels of the "normal" splicing variant in saline-injected muscles were 57% of that in the wild-type muscles. PMO injection increased the expression about 1.4-fold to 78% of that in wild-type mice. As *Clcn1* heterozygous mutant mice did not show a myotonic phenotype[34], the myotonia in HSA^{LR} mice was unlikely to have been caused by haploinsufficiency of full-length Clcn1 protein. Instead, the truncated protein translated from the exon 7A-countaining mRNA may have dominant-negative activity, since full-length Clcn1 protein functions in a dimeric form. Berg *et al.* showed that the truncated Clcn1 protein did not function as a chloride channel, but rather disturbed the channel activity of full-length Clcn1 protein[35]. In this study, expression of the splicing variant containing exon 7A was decreased by 40% in the PMO-administered group. Thus, this may have contributed to the improvement of the pathology, as well as the increased expression of the exon 7A skipping variant. The dominant-negative hypothesis suggests that the AON therapy should completely prevent exon 7A inclusion when used to treat myotonia, in contrast to Duchenne muscular dystrophy, in which the partial restoration of dystrophin expression could lead to the improvement of muscle strength.

In the course of our search for the optimal PMO sequence to correct *Clcn1* splicing, we found that 1–25 and 16–40 PMOs suppressed the inclusion of exon 7A well, but that 26–50 PMO did not. The fact that steric blocking of the 16–25 region promoted exon skipping indicates that proteins that bind to this region are essential for exon 7A recognition. Previously, we showed that the 8 nt at the 5′ end of exon 7A serve as an ESE and that an RNA-binding protein, Mbnl1, prevented the inclusion of exon 7A by binding to the ESE[29]. Unlike the ESE, the sequence of the 16–25 region was pyrimidine-rich and did not contain the Mbnl1-recognition motif, YGCY. It remains to be determined which proteins bind to the region to regulate exon 7A splicing.

In this study, we tried to cure DM1 model mice using a PMO targeted to *Clcn1*. However, considering that dozens of genes are abnormally spliced in patients with DM1, it might be impractical to treat all symptoms due to mis-splicing of such genes with AONs at the same time. DM1 is caused by expansion of the CTG repeats in the 3′ UTR region of the DMPK gene. Transcripts with these expanded repeats sequester Mbnl proteins, which regulate alternative splicing, leading to global alternative splicing dysfunction[36]. Thus, expanded CUG repeat-containing RNA must be the most important target of antisense therapy for DM1, and many groups have studied the use of CAG repeat-containing AONs to dissociate Mbnl1 proteins from CUG repeat-containing RNA. Some trials to treat DM1 model mice with CAG AONs were successful[19,37], but here again the obstacle to clinical application of the AONs was the lack of an efficient delivery method. Our ultrasound-mediated delivery system with Bubble liposomes must have a beneficial effect on the delivery of CAG-containing AONs.

Methods

AONs. Phosphorothioate 2′ *O*-methyl RNA oligonucleotides and phosphorodiamidate morpholino oligonucleotides were purchased from IDT (Coralville, IA, USA) and Gene Tools (Philomath, OR, USA), respectively. The sequences of the oligonucleotides are listed in Supplementary Table ST1. Both AONs were dissolved in water.

Construct. The *Clcn1* minigene has been described previously[29]. Briefly, a *Clcn1* minigene fragment covering exons 6 to 7 was amplified from mouse genomic DNA by PCR and inserted into the *BglII-SalI* sites of pEGFP-C1 (Clontech Laboratories, Mountain View, CA, USA).

Cellular splicing assay. COS-7 cells were cultured in Dulbecco's modified Eagle's medium (DMEM; Sigma-Aldrich, St. Louis, MO, USA) supplemented with 10% heat-inactivated fetal bovine serum (Life Technologies, Foster City, CA, USA) in a humidified atmosphere containing 5% CO_2 at 37°C.

For the splicing assay, COS-7 cells were cultured in 12-well plates and transfected with 0.1 μg of the *Clcn1* minigene and AONs (0.1 μmol) at 60–80% confluence. Polyethylenimine and Endo-Porter (Gene Tools) were used for the transfection of PS2OMe RNA and PMOs, respectively. Forty-eight hours later, total RNA was extracted from the transfected cells using a GenElute Mammalian Total RNA Miniprep Kit (Sigma-Aldrich).

Animals. HSA^{LR} mice are FVB/n-background transgenic mice that express expanded CTG repeats under the control of the human skeletal actin promoter in skeletal muscle[38]. Compared with the first established line, the number of the repeat was reduced: the mice used in this study carried 180–200 repeats. All the mutant mice showed persistent contraction of gluteal muscles after they bucked. We used FVB/nJcl mice (Clea Japan, Tokyo, Japan) as wild-type controls.

The present study was approved by the Ethical Committee for Animal Experiments at the University of Tokyo, and was carried out in accordance with the Guidelines for Research with Experimental Animals of the University of Tokyo and the NIH Guide for the Care and Use of Laboratory Animals (NIH Guide, revised 1996).

Bubble liposomes. Bubble liposomes were prepared by previously described methods[24]. Briefly, PEG liposomes composed of 1,2-dipalmitoyl-sn-glycero-3-phosphocholine (DPPC) (NOF Corporation, Tokyo, Japan) and 1,2-distearoyl-sn-glycero-3-phosphatidyl-ethanolamine-polyethyleneglycol (DSPE-PEG2000-OMe) (NOF Corporation) at a molar ratio of 94 : 6 were prepared by a reverse phase evaporation method. Briefly, all reagents were dissolved in 1 : 1 (v/v) chloroform/diisopropyl ether. Phosphate-buffered saline was added to the lipid solution, and the mixture was sonicated and then evaporated at 47°C. The organic solvent was completely removed, and the size of the liposomes was adjusted to less than 200 nm using extruding equipment and a sizing filter (pore size: 200 nm) (Nuclepore Track-Etch Membrane; Whatman Plc, Maidstone, Kent, UK). The lipid concentration was measured using a Phospholipid C test (Wako Pure Chemical Industries, Ltd, Osaka, Japan). Bubble liposomes were prepared from liposomes and perfluoropropane gas (Takachio Chemical Ind. Co. Ltd, Tokyo, Japan). First, 2-ml sterilised vials containing 0.8 ml of liposome suspension (lipid concentration: 1 mg/ml) were filled with perfluoropropane gas, capped and then pressurised with a further 3 ml of perfluoropropane gas. The vial was placed in a bath-type sonicator (38 kHz, 250 W) (SONO-CLEANER CA-4481L; Kaijo Denki, Tokyo, Japan) for 1 min to form Bubble liposomes.

Injection of morpholino oligonucleotides with Bubble liposomes and ultrasound. PMO (20 μg) and the Bubble liposome suspension (30 μl) were injected into the TA muscles of *HSA*^{LR} mice (6 weeks old) using a 30-gauge needle (NIPRO Co., Osaka, Japan). Immediately after injection, ultrasound (frequency, 1 MHz; duty, 50%; intensity, 2.0 W/cm^2; time, 60 s) was applied transdermally downstream of the injection site using a 6-mm diameter probe. A SONITRON 1000 device (Rich-Mar, Chattanooga, TN, USA) was used to generate the ultrasound. We administrated the PMO three times at weekly intervals. Three weeks after the last administration, we performed EMG measurements and then killed the mice and harvested the TA muscles for RT-PCR analysis and immunohistochemistry.

Electromyographic recording and electrical stimulation. Implantation of EMG electrodes and stimulating electrodes was carried out under aseptic conditions on mice anaesthetised with 2% vapourised isoflurane in air. Body temperature was measured rectally and was maintained at 37–38°C using a homeothermic heating pad (BioResearch Center, Aichi, Japan). Bipolar wire electrodes (tip distance, 1–2 mm) made of Teflon-insulated stainless steel wire (76 μm diameter bare, 140 μm coated; cat. no. 791000; A-M Systems, Carlsborg, WA, USA) were implanted in the TA and gastrocnemius (GA) muscles to record EMG activity. The electrical stimulation of the TA muscle was achieved using two wire electrodes that were inserted under the skin over the TA muscle and placed along the longitudinal axis of the muscle. After full recovery from the anaesthesia, alert mice were restrained in a cylindrical mouse-sized cage, with their hind limbs out of the cage to maintain their muscles at their resting lengths. The EMG signals were amplified and bandpass filtered (15 Hz–1 KHz; AB-611J; Nihon-Koden, Co., Tokyo, Japan), digitised with an analog-digital converter (PowerLab 16/30, ADInstruments Ltd, Oxford, UK) and recorded (sampling rate 10 kHz) on a computer. Electrical stimulation consisted of repetitive square pulses (train of 20 pulses at 100 Hz, 1 ms duration) delivered by an isolation unit (SS-202J; Nihon-Koden) connected to a pulse generator (SEN-3401, Nihon-Koden). The stimulus intensity was adjusted to evoke ankle dorsiflexion and avoid overt movements and animal discomfort. EMG measurements were recorded in single-blinded manner.

EMG data analysis. Myotonic EMG activities were easily confirmed by visual inspection and analysed using custom-written MATLAB software (MathWorks, Inc., Natick, MA, USA). EMG signals were full-wave-rectified and filtered with a 20 Hz low-pass second-order Butterworth filter. Offset of the EMG signal was defined as a deflection below three standard deviations from baseline. The baseline level was defined as the mean EMG signal in the resting state before stimulation. Duration of myotonic activities was defined as the period from the termination of stimulation to the offset time. Myotonic activities were integrated during the duration of myotonia and calculated by subtracting the baseline level. To quantify EMG activities per unit time, iEMG values were then calculated as the integrated myotonia value divided by corresponding net duration. The EMG data were analysed in a single-blinded manner.

RT-PCR analysis. Total RNA was extracted from TA muscles and cultured cells using TRIzol reagent (Life Technologies) and a GenElute Mammalian Total RNA Miniprep Kit (Sigma-Aldrich), respectively, according to the manufacturers' instructions.

Typically, 0.5–1.0 μg of total RNA was reverse-transcribed with a PrimeScript 1st Strand cDNA Synthesis Kit (Takara Bio, Shiga, Japan) using oligo(dT) primers. PCR reactions were performed using Ex Taq DNA polymerase (Takara Bio). The sequences of the PCR primers are listed in Supplementary Table ST2. The products were electrophoretically resolved on an 8% polyacrylamide gel that was stained with ethidium bromide and analysed using an LAS-3000 luminescence image analyser (FujiFilm, Tokyo, Japan). The ratio of exon 7A inclusion in *Clcn1* mRNA was calculated as (7A inclusion)/(7A inclusion + 7A skipping) × 100.

Immunofluorescence. Frozen sections (6 μm thick) of unfixed TA muscles were immunostained with an affinity-purified rabbit polyclonal anti-Clcn1 antibody (dilution 1 : 50; Alpha Diagnostics International, San Antonio, TX, USA). The secondary antibody was Alexa Fluor 488-conjugated goat anti-rabbit IgG (Life Technologies) used at a dilution of 1 : 600. Images were collected using an IX70 inverted microscope (Olympus, Tokyo, Japan) equipped with a ×20 objective lens. Exposure time and threshold were identical for all comparisons of antisense and saline controls.

Statistics. A two-tailed Student's *t*-test or Tukey's multiple comparison test were used for statistical comparison.

1. Aslanidis, C. *et al.* Cloning of the essential myotonic dystrophy region and mapping of the putative defect. *Nature* **355**, 548–551 (1992).
2. Brook, J. D. *et al.* Molecular basis of myotonic dystrophy: expansion of a trinucleotide (CTG) repeat at the 3′ end of a transcript encoding a protein kinase family member. *Cell* **68**, 799–808 (1992).
3. Buxton, J. *et al.* Detection of an unstable fragment of DNA specific to individuals with myotonic dystrophy. *Nature* **355**, 547–548 (1992).
4. Harley, H. G. *et al.* Expansion of an unstable DNA region and phenotypic variation in myotonic dystrophy. *Nature* **355**, 545–546 (1992).
5. Harper, P. S. *Myotonic dystrophy,* 3rd ed. (Saunders, W. B. Philadelphia, 2001).
6. Philips, A. V., Timchenko, L. T. & Cooper, T. A. Disruption of splicing regulated by a CUG-binding protein in myotonic dystrophy. *Science* **280**, 737–741 (1998).
7. Savkur, R. S., Philips, A. V. & Cooper, T. A. Aberrant regulation of insulin receptor alternative splicing is associated with insulin resistance in myotonic dystrophy. *Nat. Genet.* **29**, 40–47 (2001).
8. Fugier, C. *et al.* Misregulated alternative splicing of BIN1 is associated with T tubule alterations and muscle weakness in myotonic dystrophy. *Nat. Med.* **17**, 720–725 (2011).
9. Koebis, M. *et al.* Alternative splicing of myomesin 1 gene is aberrantly regulated in myotonic dystrophy type 1. *Genes Cells* **16**, 961–972 (2011).
10. Ohsawa, N., Koebis, M., Suo, S., Nishino, I. & Ishiura, S. Alternative splicing of PDLIM3/ALP, for alpha-actinin-associated LIM protein 3, is aberrant in persons with myotonic dystrophy. *Biochem. Biophys. Res. Commun.* **409**, 64–69 (2011).
11. Charlet, B. N. *et al.* Loss of the muscle-specific chloride channel in type 1 myotonic dystrophy due to misregulated alternative splicing. *Mol. Cell.* **10**, 45–53 (2002).
12. Mankodi, A. *et al.* Expanded CUG repeats trigger aberrant splicing of ClC-1 chloride channel pre-mRNA and hyperexcitability of skeletal muscle in myotonic dystrophy. *Mol. Cell.* **10**, 35–44 (2002).
13. Lossin, C. & George, A. L. Jr. Myotonia congenita. *Adv. Genet.* **63**, 25–55 (2008).
14. Wheeler, T. M., Lueck, J. D., Swanson, M. S., Dirksen, R. T. & Thornton, C. A. Correction of ClC-1 splicing eliminates chloride channelopathy and myotonia in mouse models of myotonic dystrophy. *J. Clin. Invest.* **117**, 3952–3957 (2007).
15. Kole, R., Krainer, A. R. & Altman, S. RNA therapeutics: beyond RNA interference and antisense oligonucleotides. *Nat. Rev. Drug. Discov.* **11**, 125–140 (2012).
16. Stein, D., Foster, E., Huang, S. B., Weller, D. & Summerton, J. A specificity comparison of four antisense types: morpholino, 2′-O-methyl RNA, DNA, and phosphorothioate DNA. *Antisense Nucleic Acid Drug Dev.* **7**, 151–157 (1997).
17. Wu, B. *et al.* Dose-dependent restoration of dystrophin expression in cardiac muscle of dystrophic mice by systemically delivered morpholino. *Gene Ther.* **17**, 132–140 (2010).
18. Wheeler, T. M. *et al.* Targeting nuclear RNA for in vivo correction of myotonic dystrophy. *Nature* **488**, 111–115 (2012).
19. Leger, A. J. *et al.* Systemic delivery of a peptide-linked morpholino oligonucleotide neutralizes mutant RNA toxicity in a mouse model of myotonic dystrophy. *Nucleic Acid Ther.* **23**, 109–117 (2013).
20. Lu, Q. L., Liang, H. D., Partridge, T. & Blomley, M. J. Microbubble ultrasound improves the efficiency of gene transduction in skeletal muscle in vivo with reduced tissue damage. *Gene Ther.* **10**, 396–405 (2003).
21. Shen, Z. P., Brayman, A. A., Chen, L. & Miao, C. H. Ultrasound with microbubbles enhances gene expression of plasmid DNA in the liver via intraportal delivery. *Gene Ther.* **15**, 1147–1155 (2008).
22. Haag, P. *et al.* Microbubble-enhanced ultrasound to deliver an antisense oligodeoxynucleotide targeting the human androgen receptor into prostate tumours. *J. Steroid Biochem. Mol. Biol.* **102**, 103–113 (2006).
23. Suzuki, R. *et al.* Gene delivery by combination of novel liposomal bubbles with perfluoropropane and ultrasound. *J. Control Release* **117**, 130–136 (2007).
24. Negishi, Y. *et al.* Delivery of an angiogenic gene into ischemic muscle by novel bubble liposomes followed by ultrasound exposure. *Pharm. Res.* **28**, 712–719 (2011).
25. Negishi, Y. *et al.* Local gene delivery system by bubble liposomes and ultrasound exposure into joint synovium. *J. Drug Deliv.* **2011**, 203986 (2011).
26. Negishi, Y. *et al.* Systemic delivery systems of angiogenic gene by novel bubble liposomes containing cationic lipid and ultrasound exposure. *Mol. Pharm.* **9**, 1834–1840 (2012).
27. Sugano, M. *et al.* Gene delivery system involving Bubble liposomes and ultrasound for the efficient in vivo delivery of genes into mouse tongue tissue. *Int. J. Pharm.* **422**, 332–337 (2012).
28. Negishi, Y. *et al.* AG73-modified Bubble liposomes for targeted ultrasound imaging of tumor neovasculature. *Biomaterials* **34**, 501–507 (2013).
29. Kino, Y. *et al.* MBNL and CELF proteins regulate alternative splicing of the skeletal muscle chloride channel CLCN1. *Nucleic Acids Res.* **37**, 6477–6490 (2009).
30. Lin, X. *et al.* Failure of MBNL1-dependent post-natal splicing transitions in myotonic dystrophy. *Hum. Mol. Genet.* **15**, 2087–2097 (2006).
31. Summerton, J. & Weller, D. Morpholino antisense oligomers: design, preparation, and properties. *Antisense Nucleic Acid Drug Dev.* **7**, 187–195 (1997).
32. Templeton, N. S. & Templeton, N. S. *Gene and cell therapy: therapeutic mechanisms and strategies.* 2nd ed. (Marcel Dekker, New York, 2004).
33. Sazani, P. *et al.* Systemically delivered antisense oligomers upregulate gene expression in mouse tissues. *Nat. Biotechnol.* **20**, 1228–1233 (2002).
34. Chen, M. F., Niggeweg, R., Iaizzo, P. A., Lehmann-Horn, F. & Jockusch, H. Chloride conductance in mouse muscle is subject to post-transcriptional compensation of the functional Cl- channel 1 gene dosage. *J. Physiol.* **504**, 75–81 (1997).
35. Berg, J., Jiang, H., Thornton, C. A. & Cannon, S. C. Truncated ClC-1 mRNA in myotonic dystrophy exerts a dominant-negative effect on the Cl current. *Neurology* **63**, 2371–2375 (2004).
36. Ranum, L. P. & Cooper, T. A. RNA-mediated neuromuscular disorders. *Annu. Rev. Neurosci.* **29**, 259–277 (2006).

37. Wheeler, T. M. *et al.* Reversal of RNA dominance by displacement of protein sequestered on triplet repeat RNA. *Science* **325**, 336–339 (2009).
38. Mankodi, A. *et al.* Myotonic dystrophy in transgenic mice expressing an expanded CUG repeat. *Science* **289**, 1769–1773 (2000).

Acknowledgements

We thank Prof. Charles A. Thornton (University of Rochester) for providing us *HSA*^{LR} mice. We also thank Dr H. Mitsuhashi for valuable discussions and encouragement. This work was supported in part by the Comprehensive Research on Disability Health and Welfare, from the Ministry of Health, Labour and Welfare Japan, and Intramural Research Grant (23–5) for Neurological and Psychiatric Disorders of NCNP.

Author contributions

S.I. conceived the project. M.K. designed the experiments. T.K. carried out cell culture-based splicing assay. K.N., M.P.T. carried out the delivery of PMO. R.M., Y.H. and I.N. carried out histochemical staining. H.Y., M.H., M.S. and D.Y. designed and carried out EMG analysis. Y.N. and Y.E.-T. prepared Bubble liposomes.

Additional information

Supplementary Information accompanies this paper at http://www.nature.com/scientificreports

Competing financial interests: The authors declare no competing financial interests.

How to cite this article: Koebis, M. *et al.* Ultrasound-enhanced delivery of Morpholino with Bubble liposomes ameliorates the myotonia of myotonic dystrophy model mice. *Sci. Rep.* **3**, 2242; DOI:10.1038/srep02242 (2013).

A Kir3.4 mutation causes Andersen–Tawil syndrome by an inhibitory effect on Kir2.1

Yosuke Kokunai, MD, PhD*
Tomohiko Nakata, MD*
Mitsuru Furuta, MD*
Souhei Sakata, PhD
Hiromi Kimura, MD, PhD
Takeshi Aiba, MD, PhD
Masao Yoshinaga, MD, PhD
Yusuke Osaki, MD
Masayuki Nakamori, MD, PhD
Hideki Itoh, MD, PhD
Takako Sato, MD, PhD
Tomoya Kubota, MD, PhD
Kazushige Kadota, MD, PhD
Katsuro Shindo, MD, PhD
Hideki Mochizuki, MD, PhD
Wataru Shimizu, MD, PhD
Minoru Horie, MD, PhD
Yasushi Okamura, MD, PhD
Kinji Ohno, MD, PhD
Masanori P. Takahashi, MD, PhD

Correspondence to Dr. Takahashi: mtakahas@neurol.med.osaka-u.ac.jp

Supplemental data at Neurology.org

ABSTRACT

Objective: To identify other causative genes for Andersen–Tawil syndrome, which is characterized by a triad of periodic paralysis, cardiac arrhythmia, and dysmorphic features. Andersen–Tawil syndrome is caused in a majority of cases by mutations in *KCNJ2*, which encodes the Kir2.1 subunit of the inwardly rectifying potassium channel.

Methods: The proband exhibited episodic flaccid weakness and a characteristic TU-wave pattern, both suggestive of Andersen–Tawil syndrome, but did not harbor *KCNJ2* mutations. We performed exome capture resequencing by restricting the analysis to genes that encode ion channels/associated proteins. The expression of gene products in heart and skeletal muscle tissues was examined by immunoblotting. The functional consequences of the mutation were investigated using a heterologous expression system in *Xenopus* oocytes, focusing on the interaction with the Kir2.1 subunit.

Results: We identified a mutation in the *KCNJ5* gene, which encodes the G-protein–activated inwardly rectifying potassium channel 4 (Kir3.4). Immunoblotting demonstrated significant expression of the Kir3.4 protein in human heart and skeletal muscles. The coexpression of Kir2.1 and mutant Kir3.4 in *Xenopus* oocytes reduced the inwardly rectifying current significantly compared with that observed in the presence of wild-type Kir3.4.

Conclusions: We propose that *KCNJ5* is a second gene causing Andersen–Tawil syndrome. The inhibitory effects of mutant Kir3.4 on inwardly rectifying potassium channels may account for the clinical presentation in both skeletal and heart muscles. ***Neurology*® 2014;82:1–7**

GLOSSARY

cRNA = complementary RNA; **LQT** = long QT; **SNP** = single nucleotide polymorphism; **SNV** = single nucleotide variant.

Periodic paralysis is a heterogeneous disorder caused by mutations in several ion channel genes, including sodium, calcium, and potassium channels.[1–3] Andersen–Tawil syndrome is a form of periodic paralysis that is characterized by a triad of periodic muscle weakness, cardiac arrhythmia, and dysmorphic features.[4,5] Although dominantly inherited, its phenotypes are highly variable and its penetrance is low.[6,7] The syndrome has been proposed as LQT7; however, the ECG features are distinct from those of classic forms of long QT (LQT) syndrome, i.e., characteristic TU patterns, including enlarged U waves, a wide TU junction, and a prolonged terminal T-wave downslope.[6,8]

KCNJ2 mutation, which encodes the Kir2.1 subunit, causes Andersen–Tawil syndrome.[9] Kir2.1 is predominantly expressed in the brain, heart, and skeletal muscles and forms an inwardly rectifying potassium channel via the homo- or heteromeric assembly of 4 Kir2.x subunits.[10] Most *KCNJ2* mutations cause loss of function or dominant-negative suppression of the inwardly rectifying

*These 3 authors contributed equally to this work.

From the Department of Neurology (Y.K., M.F., M.N., T.K., H.M., M.P.T.), and Laboratory of Integrative Physiology, Department of Physiology (S.S., Y. Okamura), Osaka University Graduate School of Medicine, Suita, Osaka; Division of Neurogenetics (T.N., K.O.), Center for Neurological Diseases and Cancer, Nagoya University Graduate School of Medicine, Nagoya, Aichi; Department of Cardiovascular and Respiratory Medicine (H.K., H.I., M.H.), Shiga University of Medical Science, Otsu, Shiga; Division of Arrhythmia and Electrophysiology (T.A., W.S.), Department of Cardiovascular Medicine, National Cerebral and Cardiovascular Center, Suita, Osaka; Department of Pediatrics (M.Y.), National Hospital Organization Kagoshima Medical Center, Kagoshima; Department of Neurology (Y. Osaki, K.S.), Kurashiki Central Hospital, Kurashiki, Okayama; Department of Legal Medicine (T.S.), Osaka Medical College, Takatsuki, Osaka; Department of Cardiology (K.K.), Kurashiki Central Hospital, Kurashiki, Okayama; and Department of Cardiovascular Medicine (W.S.), Nippon Medical School, Bunkyo, Tokyo, Japan. Y.K. is currently affiliated with the Department of Neurology, Osaka General Medical Center, Sumiyoshi, Osaka, Japan; and T.K. is currently affiliated with the Department of Biochemistry and Molecular Biology, Division of Biological Sciences, The University of Chicago, IL.

Go to Neurology.org for full disclosures. Funding information and disclosures deemed relevant by the authors, if any, are provided at the end of the article.

potassium current that stabilizes excitability during the terminal phase of repolarization in the heart and the resting membrane potential in skeletal muscle.[11]

Approximately 40% patients with Andersen–Tawil syndrome do not harbor mutations in *KCNJ2*, suggesting the presence of other causative genes.[12] We identified a patient with periodic paralysis and characteristic ECG features suggestive of Andersen–Tawil syndrome but failed to find mutations in *KCNJ2*. Exome capture resequencing analysis revealed a novel mutation in *KCNJ5*. We investigated the functional consequences of the mutation using a heterologous expression system in *Xenopus* oocytes to understand its pathomechanism.

Figure 1 **Pedigree of the family and ECG recordings of the proband**

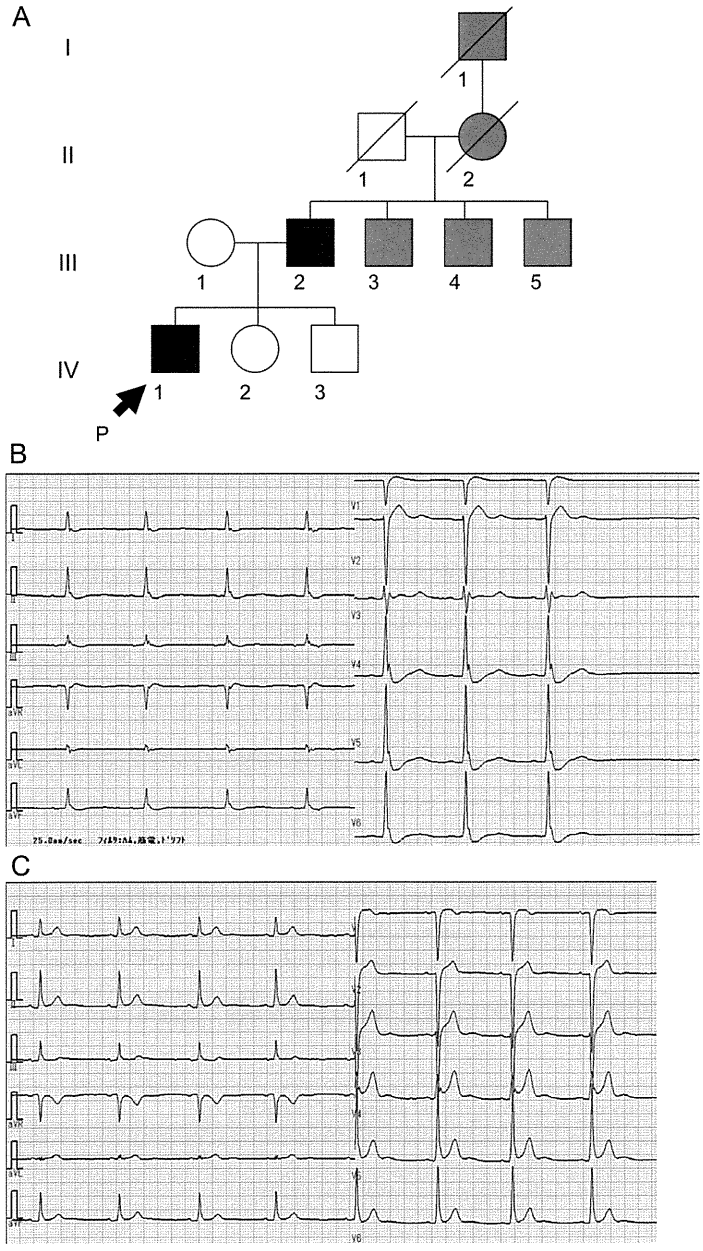

(A) Pedigree of the family. Filled symbols represent affected and empty symbols represent unaffected individuals. Gray symbols represent patients with arrhythmia lacking detailed information. DNA was available only from the proband. ECG recordings of the proband during the attack of hypokalemic periodic paralysis (B) and at the interictal state (C). In addition to prominent U waves, atrial standstill was also observed during the paralytic attack (B).

METHODS

Patient. The proband (IV-1 in figure 1A) was a 35-year-old man who experienced periodic episodes of paralysis with reduced serum potassium concentrations starting at the age of 31 years. The episodes occurred several times in a year and lasted from 1 to 10 days. During a severe attack, the weakness, which initially manifested in the legs, extended to the upper limbs within several days and then gradually improved. The proband showed an abnormal decrement in the amplitude of compound motor action potentials in the prolonged exercise test at the interictal state. He showed no dysmorphic features, but had a family history of arrhythmia (figure 1A). The clinical data of other family members were not available because of lack of consent. His father (III-2) underwent pacemaker implantation because of bradycardia/tachycardia syndrome with atrial fibrillation. Three uncles, a grandmother, and a great-grandfather, all on his father's side, had arrhythmia; however, the details of their conditions were not available. Within the knowledge of the proband, no other family members had experience of paralytic attacks. F1

The proband had no cardiac symptoms, but the ECG recorded during the paralytic attack with a serum potassium concentration of 2.0 mEq/L exhibited prominent U waves and possible sinus arrest (figure 1C, left). The U waves were consistently observed at normal potassium concentration (figure 1C, right). His thyroid function was normal and he did not show hypertension or increased plasma aldosterone levels, which ruled out primary hyperaldosteronism.

Standard protocol approvals, registrations, and patient consents. We obtained informed consent from the patient using protocols approved by the Institutional Ethics Review Board of Osaka University.

Sanger sequencing. Genomic DNA was extracted from blood leukocytes. The regions encompassing known causative mutations for periodic paralysis in *SCN4A* and *CACNA1S* and the entire coding region of *KCNJ2* and *KCNJ18* were amplified using either Platinum Taq DNA Polymerase High Fidelity (Life Technologies, Carlsbad, CA) or the Advantage-GC2 PCR kit (Clontech, Mountain View, CA) (primer sequences are listed in table e-1 on the *Neurology*® Web site at Neurology.org).[13] The purified fragments were sequenced using an automated DNA sequencer (Big Dye Terminator version 3.1 and ABI3100; Life Technologies).

Exome capture resequencing analysis. We enriched exonic regions of genomic DNA using the SureSelect Human All Exon v.2 kit (Agilent Technologies, Santa Clara, CA), which covers 44 mega base pairs of the human genome or 98.2% of the CCDS (Consensus Coding Sequence) database and sequenced 50 base pairs of each tag in a single direction using the SOLiD 4 system (Life Technologies). We obtained 80.0 $\times$ 10^6 tags of 50–base pair reads and mapped 57.7 $\times$ 10^6 tags (72.1%) to the hg19/GRCh37 human genome, which yielded a mean coverage of 53.2 on the targeted exome regions. Next, we removed multiple-aligned reads,

unreliable reads, and PCR duplicates using Avadis NGS 1.3 (Strand, San Francisco, CA). Single nucleotide variants (SNVs) and indels were called by Avadis NGS using default parameters. We restricted our analysis to 162 genes that encode ion channels and associated proteins (table e-2). We then excluded SNVs and indels that were registered in the nonclinical subset of dbSNP137, 1000 Genomes database, 6,500 genomes in the NHLBI ESP database (http://evs.gs.washington.edu/EVS/), or our cohort of 38 other diseases and controls. The other diseases in our cohort included congenital myasthenic syndromes, osteogenesis imperfecta, mitochondrial myopathies, and Schwartz–Jampel syndrome.

Immunoblotting. Skeletal muscle and heart tissues were taken at autopsy from control patients with disease (myotonic dystrophy type 1 and amyotrophic lateral sclerosis). Tissues were homogenized in a 10× volume of radioimmunoprecipitation assay buffer (25 mM Tris-HCl; pH 7.5; 150 mM NaCl; 1% NP-40; 1% sodium deoxycholate; and 0.1% sodium dodecyl sulfate) containing a protein inhibitor cocktail (Sigma-Aldrich, St. Louis, MO). The homogenate was centrifuged for 10 minutes at 10,000*g* and the supernatant was collected. Equal amounts of protein (20 μg) were separated by sodium dodecyl sulfate–polyacrylamide gel electrophoresis and transferred onto Immobilon-P membranes (Millipore, Bedford, MA), as previously described.[14] Blots were blocked for nonspecific protein binding with 5% (w/v) nonfat milk overnight and then incubated at room temperature for 1 hour with a 1:3,000-diluted antibody against Kir3.4 (AVIVA Systems Biology, Atlanta, GA) or GAPDH (glyceraldehyde 3-phosphate dehydrogenase) (Sigma-Aldrich). After repeated washings, the membranes were incubated at room temperature for 1 hour with peroxidase-conjugated goat anti-rabbit immunoglobulin G (1:30,000 dilution; GE Healthcare Biosciences, Pittsburgh, PA). The membranes were then washed, developed using an enhanced chemiluminescence kit (GE Healthcare Biosciences), and exposed to x-ray film.

Electrophysiology. Complementary RNAs (cRNAs) for mouse IRK1, which differs from human Kir2.1 by only 5 amino acids, and human Kir3.4 were expressed in *Xenopus* oocytes. Complementary DNAs cloned into the pGEMHE vector were kindly provided by Dr. Diomedes Logothetis (Virginia Commonwealth University). A site-directed mutagenesis kit (KOD-Plus Mutagenesis Kit; Toyobo, Osaka, Japan) was used to introduce the G387R mutation into the human Kir3.4 clone. The cRNAs were synthesized from linearized plasmid DNA using an mMESSAGE mMACHINE transcription kit (Life Technologies).

Xenopus oocytes were collected from frogs anesthetized in water containing 0.2% ethyl 3-aminobenzoate methanesulfonate salt (Sigma-Aldrich). The oocytes were isolated and defolliculated by treatment with type I collagenase (1.0 mg/mL; Sigma-Aldrich) and then injected with cRNAs that were quantified using a spectrophotometer (NanoDrop 2000; Thermo Fisher, Wilmington, DE). Injected oocytes were incubated for 2 to 3 days at 18°C in ND96 solution (5 mM HEPES; 96 mM NaCl; 2 mM KCl; 1.8 mM $CaCl_2$; and 1 mM $MgCl_2$; pH 7.5; supplemented with gentamicin and pyruvate).

Macroscopic currents were recorded with a 2-electrode voltage clamp using a bath-clamp amplifier (OC-725C; Harvard Apparatus, Holliston, MA). Stimulation, data acquisition, and data analysis were performed using the Patchmaster software (HEKA Elektronic, Lambrecht/Pfalz, Germany). Glass microelectrodes were filled with 3 M KCl, with a final resistance ranging from 0.2 to 1.0 MΩ. Recordings were performed at room temperature (22°C–25°C) in a bath solution containing 90 mM KCl, 3 mM $MgCl_2$, and 5 mM HEPES (pH 7.35–7.4). Step pulses ranging from −150 to +50 mV were applied from a holding potential of 0 mV for 200 milliseconds.

RESULTS Genome analyses of the proband. Genome samples from other members of the family were not available. Sanger nucleotide sequence analysis of the patient's DNA showed no causative mutations in *SCN4A* and *CACNA1S* (which were previously reported as being responsible for periodic paralysis) or in the entire coding region of *KCNJ2* and *KCNJ18*. Furthermore, an intragenic deletion or duplication in *KCNJ2* was excluded by the multiplex ligation-dependent probe amplification method (e-Methods and figure e-1).

The exome capture resequencing analysis yielded 44,550 SNVs and 1,852 indels. We restricted our analysis to 162 genes that encode ion channels and associated proteins (table e-2) and then excluded SNVs and indels registered in public single nucleotide polymorphism (SNP) databases (nonclinical subset of dbSNP137, 1000 Genomes database, and 6,500 genomes in the NHLBI ESP database) or our cohort of 38 other diseases and controls, which resulted in the identification of 3 heterozygous missense SNVs (table 1). Direct sequencing of T1
the 3 SNVs by the Sanger method revealed that the SNVs in *RABGEF1* and *KCNT1* were artifacts, whereas the SNV in *KCNJ5*, G387R, was truly heterozygous in the patient. *KCNJ5* encodes a G-protein–activated inwardly rectifying potassium channel 4 (Kir3.4). Glycine at position 387 in the Kir3.4 is located at the C-terminus and is highly conserved across species, including mammals, chickens, and zebra fish. The G387R mutation was previously reported in a single Chinese family with LQT syndrome but absent in 528 controls.[15]

Table 1 Heterozygous SNVs called by Avadis NGS in 162 genes encoding ion channels and associated proteins

Chr.	Pos.	Gene	Ex.	SNVs	a.a.	Description	Variants/total[a]
chr7	66,270,306	*RABGEF1*	8	1,100 A/G	N334D[b]	RAB guanine nucleotide exchange factor (GEF) 1	8/54
chr9	138,656,938	*KCNT1*	12	1,097 A/G	H366R[b]	Potassium channel, subfamily T, member 1	6/26
chr11	128,786,525	*KCNJ5*	3	1,159 G/C	G387R	Potassium inwardly-rectifying channel, subfamily J, member 5	44/50

Abbreviations: a.a. = predicted amino acid substitution; Chr. = chromosome; Ex. = exon number; Pos. = position according to hg19/GRCh37; SNVs = single nucleotide variants.
[a] Number of variants and total reads after eliminating multiple-aligned reads, unreliable reads, and PCR duplicates.
[b] False SNV calls that were not detected by Sanger sequencing.

Exome capture resequencing analysis covered the entire coding regions of *CACNA1S* 96.8-fold and *SCN4A* 54.4-fold on average. Two short segments of *SCN4A* were not covered by exome analysis and were directly sequenced by the Sanger method. These analyses detected a heterozygous synonymous G>A SNP, rs200175006, in *SCN4A*, which has a minor allelic frequency of 0.05% in normal population.

Immunoblotting. As mentioned above, the G387R mutation in the *KCNJ5* gene was previously identified in a family with LQT syndrome; however, no skeletal muscle features were described in that family.[15] The mutated Kir3.4 subunit has been reported to exert dominant-negative effects on Kir3.1/Kir3.4 channel complexes.[15] In the heart, Kir3.4 assembled with Kir3.1 forms an I_{KACh} current, which is predominantly expressed in the sinoatrial node and atria and contributes to the regulation of heart beat by acetylcholine; however, the function of G-protein–activated inwardly rectifying potassium channels in skeletal muscles has not been determined. Therefore, we investigated the existence and role of the Kir3.4 channel in skeletal muscle.

Figure 2 **Immunoblot of Kir3.4 in cardiac and skeletal muscle**

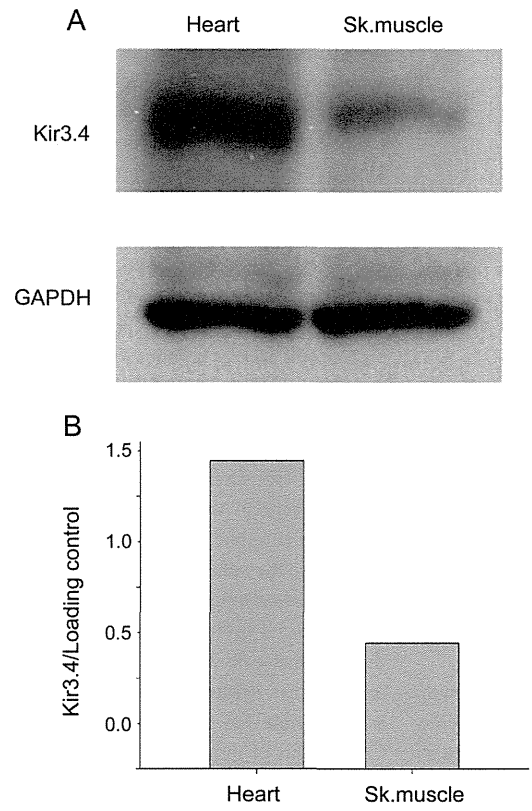

(A) Immunoblot analyses of the Kir3.4 subunit protein in the human heart and skeletal muscles are shown with loading control (GAPDH). (B) The densities of the Kir3.4 band were quantified and normalized to that of the loading control. GAPDH = glyceraldehyde 3-phosphate dehydrogenase; Sk. = skeletal.

Because messenger RNA for *KCNJ5* was detected in skeletal muscle tissue using an expression microarray assay, we tested whether the Kir3.4 protein is expressed in human skeletal muscles with immunoblotting, which revealed significant expression of the Kir3.4 protein in skeletal muscle from patients with myotonic dystrophy (figure 2) and amyotrophic lateral sclerosis (data not shown). F2

Electrophysiology. Although we found significant expression of Kir3.4 protein in human skeletal muscles, a significant G-protein–activated inwardly rectifying potassium current has never been physiologically recorded in mammalian skeletal muscles. Our patient exhibited clinical features that were indistinguishable from those of Andersen–Tawil syndrome, which is caused by loss-of-function mutations of *KCNJ2*; therefore, we suspected that mutated Kir3.4 may assemble heteromerically with Kir2.1, which is encoded by *KCNJ2*, thereby inhibiting inwardly rectifying potassium currents. Injection of Kir2.1 cRNA into oocytes induced a robust expression of strong inwardly rectifying potassium currents with a fast activation on hyperpolarization. Coinjection of Kir2.1 and Kir3.4 cRNAs did not change the properties of inward rectification (figure 3A). The F3 coexpression of Kir2.1 with mutant Kir3.4 yielded a significant reduction in the inwardly rectifying potassium current compared with that observed for the coexpression of Kir2.1 with wild-type Kir3.4 (figure 3A). This reduction was observed at both conditions where cRNAs of Kir2.1 and Kir3.4 were injected with equal amounts and the amount of Kir2.1 cRNA was 10-fold greater than that of Kir3.4 (figure 3B). When wild-type or mutant Kir3.4 cRNA was injected without Kir2.1 cRNA, inwardly rectifying currents were observed; however, the amplitude of the currents was considerably smaller than that by Kir2.1 cRNA injection. These results suggest that the coexpression of mutant Kir3.4 subunits reduces inwardly rectifying potassium currents in the skeletal muscle, thus causing periodic paralysis.

***KCNJ5* gene analysis in a large cohort.** We performed Sanger sequencing analysis for mutations in *KCNJ5* in 3 Japanese cohorts of possible Andersen–Tawil syndrome, in which 46 families harbor *KCNJ2* mutations (see table e-1 for the primer sequences). Within 21 *KCNJ2*-negative cases, we identified a mutation of T158A (c.472A>G) in a single case, which originally showed prolonged QU on an ECG recorded at normal serum potassium concentration and later developed a hypokalemic paralytic attack and primary aldosteronism after 2 years.

DISCUSSION Using the exome capture resequencing analysis, we identified a *KCNJ5* mutation (which encodes the Kir3.4 subunit) in a patient with episodic

Figure 3 **Electrophysiologic studies of the mutant Kir3.4 channel using *Xenopus* oocytes**

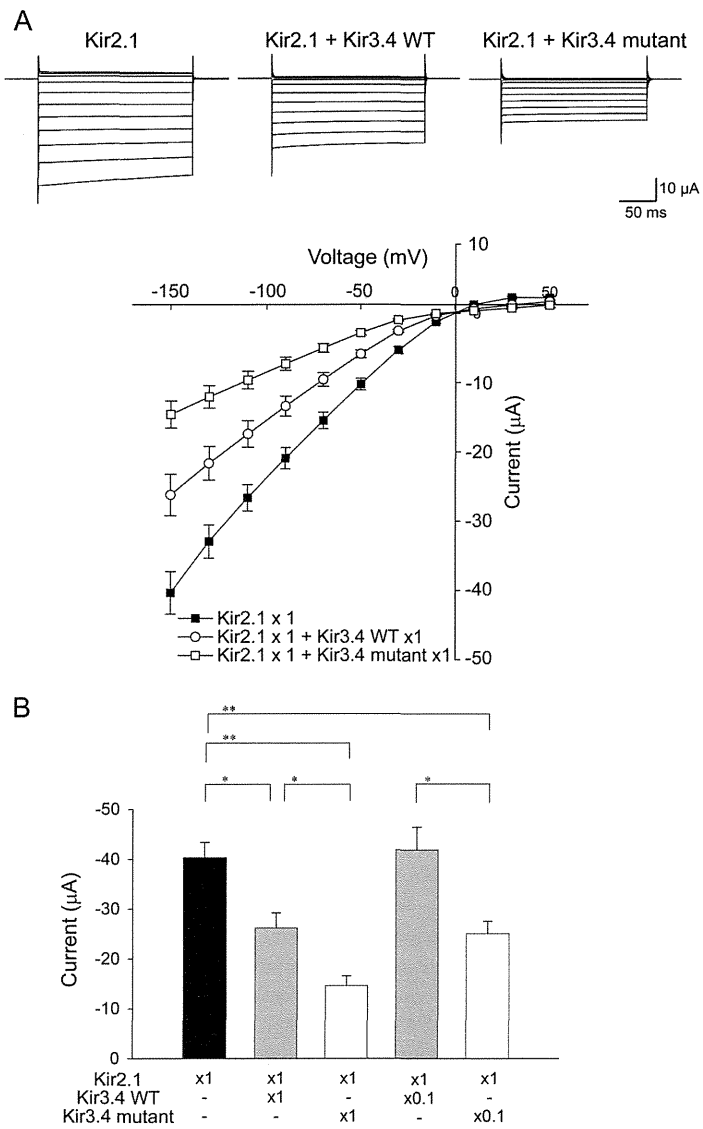

(A) Current-voltage relationships measured using step pulses for 200 milliseconds from −150 to +50 mV are shown. Symbols with error bars indicate the mean ± SEM (n = 20 for Kir2.1; 19 for Kir2.1 + Kir3.4 WT; 12 for Kir2.1 + Kir3.4 mutant). Representative current traces are shown at the top. The amount of complementary RNA (cRNA) injected into the oocytes was 3.4 ng per construct. (B) The currents induced by −150 mV step pulses are shown as a bar graph. Error bars indicate the mean ± SEM (n = 20, 19, 12, 21, and 15). The amount of cRNA for each construct was 3.4 ng for "×1" and 0.34 ng for "×0.1." *$p < 0.01$, **$p < 0.001$ (2-tailed unpaired *t* test). WT = wild type.

flaccid weakness and a characteristic TU-wave pattern, which are both suggestive of Andersen–Tawil syndrome. His family members presented autosomal-dominantly inherited arrhythmia, but apparent episodes of paralysis were observed only in the proband. The dysmorphic features did not appear to be present in any of the family members, including the proband. Although the syndrome was defined as a triad of potassium-sensitive periodic paralysis, ventricular dysrhythmias, and dysmorphic features, the paralytic attacks and dysmorphic features might not always be observed in Andersen–Tawil syndrome. It has been reported that the phenotypes are highly variable and the penetrance is not high in the *KCNJ2*-related Andersen–Tawil syndrome.[7]

It has been shown that Kir3.4 can form heteromeric channels with Kir2.1 when heterologously expressed in HEK293 cells or *Xenopus* oocytes.[16] There are no reports of the heteromerization of Kir3.4 with the Kir2.1 subunit in "native tissues"; however, Kir3.4 may have an effect on the inwardly rectifying potassium current. Reduction of the inwardly rectifying potassium current by the mutant Kir3.4 supports the notion that Kir3.4 modulates Kir2.1 and explains the clinical presentations in both skeletal and heart muscles in our case.

The G387R mutation of Kir3.4 was previously identified in a Chinese family presenting with LQT syndrome. In addition, the functional defect of the channel was characterized,[15] but the mechanism underlying the QT prolongation remained obscure. In the heart, it is known that the Kir3.4 subunit, mostly by heteromeric assembly with the Kir3.1 subunit, forms I_{KACh} channels, which are responsible for acetylcholine-dependent slowing of the heart rate. In fact, Kir3.4 knockout mice have an inability to regulate their heart rate in response to parasympathetic stimulation.[17,18] Therefore, it was initially unexpected that the decrease in I_{KACh}, which are predominantly expressed in atria, causes a defect in ventricular conductivity. The Kir2.1 subunit forms an inwardly rectifying potassium channel that provides repolarization during the most terminal phase of repolarization in ventricular cells. A suppression of inwardly rectifying potassium channels by the mutant Kir3.4 observed in *Xenopus* oocytes, if occurs in vivo, will cause a delay in the repolarization of ventricular cells and result in a prolonged QT (U) interval in ECG. Compared with other classic LQT syndromes, the prominent U wave is a hallmark of ECG findings in Andersen–Tawil syndrome caused by mutations of Kir2.1.[6,8] The similar U waves observed in our case may also support the alteration of inwardly rectifying potassium currents.

Despite the small density or absence of I_{KACh} current in skeletal muscles, we found significant expression of Kir3.4 protein in skeletal muscles. Because of the minimal role of I_{KACh} in skeletal muscle, it is unlikely that reduced I_{KACh} due to Kir3.4 mutation is responsible for the episodes of flaccid weakness. Coinjection of mutant Kir3.4 with the Kir2.1 subunit in *Xenopus* oocytes showed a reduction in the inwardly rectifying potassium current. The decrease in the inwardly rectifying potassium current caused by loss-of-function mutation in *KCNJ2* is the underlying mechanism of the episodic paralysis observed

in Andersen–Tawil syndrome.[11] Although additional evidence is necessary, the Kir3.4 subunit in skeletal muscle may have a role in regulating the size of inwardly rectifying potassium currents.

It should be noted that germline and somatic mutations in *KCNJ5* have recently been reported to be responsible for familial hyperaldosteronism and aldosterone-producing adenomas, respectively.[19] Of interest, the other mutation of *KCNJ5* (T158A), which we identified in our cohort of possible Andersen–Tawil syndrome has previously been described as a germline mutation associated with familial hyperaldosteronism.[19] Although familial hyperaldosteronism is one of the causes of secondary hypokalemic periodic paralysis, it is unlikely that the clinical phenotypes of our cases are merely the consequences of hyperaldosteronism. Laboratory data in our case with the G387R mutation did not support the presence of hyperaldosteronism, and the TU complex in our case with the T158A mutation persisted at a normal concentration of serum potassium. Although further studies are required, some mutations of *KCNJ5* may show an overlapping phenotype with familial hyperaldosteronism and Andersen–Tawil syndrome.

In this study, we have identified a novel causative gene for Andersen–Tawil syndrome, *KCNJ5*, which encodes the Kir3.4 subunit, using an exome capture resequencing analysis. The mutant Kir3.4 subunit exerted an inhibitory effect on the inwardly rectifying potassium current, likely via heteromerization with Kir2.1. Although the heteromerization of Kir2.1 with the Kir3.4 subunit in native tissues should be further clarified, our case suggests that this mechanism has a role under both physiologic and pathologic conditions in skeletal muscle and the heart.

AUTHOR CONTRIBUTIONS

Dr. Yosuke Kokunai: designing experiments, acquisition of data. Dr. Tomohiko Nakata: acquisition of data. Dr. Mitsuru Furuta: acquisition of data, revising the manuscript. Dr. Souhei Sakata: designing experiments, acquisition of data. Dr. Hiromi Kimura, Dr. Takeshi Aiba, Dr. Masao Yoshinaga, and Dr. Yusuke Osaki: acquisition of data. Dr. Masayuki Nakamori: acquisition of data, drafting the manuscript. Dr. Hideki Itoh: analysis of data. Dr. Takako Sato: acquisition of data. Dr. Tomoya Kubota: drafting/revising the manuscript. Dr. Katsushige Kadota and Dr. Katsuro Shindo: acquisition of data. Dr. Hideki Mochizuki: revising the manuscript. Dr. Wataru Shimizu: acquisition of data. Dr. Minoru Horie: designing experiments, interpretation of data, and drafting/revising the manuscript. Dr. Yasushi Okamura: designing experiments, interpretation of data, and revising the manuscript. Dr. Kinji Ohno: designing experiments, interpretation of data, and drafting/revising the manuscript. Dr. Masanori P. Takahashi: study concept or design, designing experiments, interpretation of data, and drafting/revising the manuscript.

ACKNOWLEDGMENT

The authors thank Dr. Diomedes Logothetis for kindly providing the IRK1 and Kir3.4 plasmids, Drs. Hisako Katayama and Takekazu Ohi for referring the patient, and Ms. Kimie Hayashi for her technical assistance.

STUDY FUNDING

Supported by research grants from the Ministry of Health, Labour and Welfare, Intramural research grant (23-5) of the National Center of Neurology and Psychiatry, and grants-in-aid from the Japan Society for the Promotion of Science (to K.O. and M.P.T.).

DISCLOSURE

Y. Kokunai, T. Nakata, M. Furuta, S. Sakata, H. Kimura, T. Aiba, M. Yoshinaga, Y. Osaki, M. Nakamori, H. Itoh, T. Sato, T. Kubota, K. Kadota, K. Shindo, H. Mochizuki, W. Shimizu, M. Horie, and Y. Okamura report no disclosures relevant to the manuscript. K. Ohno and M. Takahashi received funding from the Ministry of Health, Labour and Welfare of Japan, National Center of Neurology and Psychiatry, and Japan Society for the Promotion of Science. Go to Neurology.org for full disclosures.

Received June 9, 2013. Accepted in final form December 16, 2013.

REFERENCES

1. Raja Rayan DL, Hanna MG. Skeletal muscle channelopathies: nondystrophic myotonias and periodic paralysis. Curr Opin Neurol 2010;23:466–476.
2. Venance SL, Cannon SC, Fialho D, et al. The primary periodic paralyses: diagnosis, pathogenesis and treatment. Brain 2006;129:8–17.
3. Jurkat-Rott K, Lehmann-Horn F. Paroxysmal muscle weakness: the familial periodic paralyses. J Neurol 2006; 253:1391–1398.
4. Tawil R, Ptacek LJ, Pavlakis SG, et al. Andersen's syndrome: potassium-sensitive periodic paralysis, ventricular ectopy, and dysmorphic features. Ann Neurol 1994;35: 326–330.
5. Andersen ED, Krasilnikoff PA, Overvad H. Intermittent muscular weakness, extrasystoles, and multiple developmental anomalies: a new syndrome? Acta Paediatr Scand 1971;60:559–564.
6. Tristani-Firouzi M, Jensen JL, Donaldson MR, et al. Functional and clinical characterization of KCNJ2 mutations associated with LQT7 (Andersen syndrome). J Clin Invest 2002;110:381–388.
7. Kimura H, Zhou J, Kawamura M, et al. Phenotype variability in patients carrying KCNJ2 mutations. Circ Cardiovasc Genet 2012;5:344–353.
8. Zhang L, Benson DW, Tristani-Firouzi M, et al. Electrocardiographic features in Andersen-Tawil syndrome patients with KCNJ2 mutations: characteristic T-U-wave patterns predict the KCNJ2 genotype. Circulation 2005; 111:2720–2726.
9. Plaster NM, Tawil R, Tristani-Firouzi M, et al. Mutations in Kir2.1 cause the developmental and episodic electrical phenotypes of Andersen's syndrome. Cell 2001;105:511–519.
10. Zobel C, Cho HC, Nguyen TT, et al. Molecular dissection of the inward rectifier potassium current (IK1) in rabbit cardiomyocytes: evidence for heteromeric co-assembly of Kir2.1 and Kir2.2. J Physiol 2003;550:365–372.
11. Tristani-Firouzi M, Etheridge SP. Kir 2.1 channelopathies: the Andersen-Tawil syndrome. Pflugers Arch 2010;460: 289–294.
12. Donaldson MR, Yoon G, Fu YH, Ptacek LJ. Andersen-Tawil syndrome: a model of clinical variability, pleiotropy, and genetic heterogeneity. Ann Med 2004;36(suppl 1): 92–97.
13. Ryan DP, da Silva MR, Soong TW, et al. Mutations in potassium channel Kir2.6 cause susceptibility to thyrotoxic hypokalemic periodic paralysis. Cell 2010;140:88–98.
14. Nakamori M, Kimura T, Fujimura H, Takahashi MP, Sakoda S. Altered mRNA splicing of dystrophin in type 1 myotonic dystrophy. Muscle Nerve 2007;36:251–257.
15. Yang Y, Liang B, Liu J, et al. Identification of a Kir3.4 mutation in congenital long QT syndrome. Am J Hum Genet 2010;86:872–880.

16. Ishihara K, Yamamoto T, Kubo Y. Heteromeric assembly of inward rectifier channel subunit Kir2.1 with Kir3.1 and with Kir3.4. Biochem Biophys Res Commun 2009;380:832–837.
17. Wickman K, Nemec J, Gendler SJ, Clapham DE. Abnormal heart rate regulation in GIRK4 knockout mice. Neuron 1998;20:103–114.
18. Kovoor P, Wickman K, Maguire CT, et al. Evaluation of the role of I(KACh) in atrial fibrillation using a mouse knockout model. J Am Coll Cardiol 2001;37:2136–2143.
19. Choi M, Scholl UI, Yue P, et al. K+ channel mutations in adrenal aldosterone-producing adenomas and hereditary hypertension. Science 2011;331:768–772.

Clinical Neurology and Neurosurgery 115 (2013) 603–606

Contents lists available at SciVerse ScienceDirect

Clinical Neurology and Neurosurgery

journal homepage: www.elsevier.com/locate/clineuro

Muscle biopsy findings predictive of malignancy in rare infiltrative dermatomyositis

Makoto Uchino[a,b,*,1], Satoshi Yamashita[a,1], Katsuhisa Uchino[a,1], Akira Mori[a,1], Akio Hara[a,1], Tomohiro Suga[a], Tomoo Hirahara[a], Tatsuya Koide[a,b], En Kimura[a], Taro Yamashita[a], Akihiko Ueda[a], Ryoichi Kurisaki[a], Junko Suzuki[a], Shoji Honda[a], Yasushi Maeda[a], Teruyuki Hirano[a], Yukio Ando[a]

[a] Department of Neurology, Faculty of Life Sciences, Kumamoto University, 1-1-1 Honjo, Kumamoto 860-0811, Japan
[b] Department of Neurology, Jonan Hospital, Mubanchi Jonanmachi, Kumamoto 861-4214, Japan

ARTICLE INFO

Article history:
Received 26 September 2011
Received in revised form 19 April 2012
Accepted 14 July 2012
Available online 22 August 2012

Keywords:
Dermatomyositis
Polymyositis
Muscle biopsy findings
Malignancy
Rare-infiltrative type

ABSTRACT

Objective: The characteristic pathological muscular findings of polymyositis (PM) and dermatomyositis (DM) have been shown to reflect their different pathogeneses. Here, we characterized the muscle biopsy findings of PM and DM patients with or without malignancy.
Methods: We evaluated the muscle biopsy findings of 215 consecutive PM and DM patients admitted to our hospital between 1970 and 2009. Pathology of the lesion biopsy sections was classified into 3 types: endomysial infiltration-type, perivascular infiltration-type, and rare-infiltrative-type.
Results: There was no difference between the muscle pathology of PM patients with and without malignancy. However, the incidence of rare-infiltrative type muscle pathology in DM patients with malignancy was significantly higher than in those without such tumors ($p = 0.0345$).
Conclusion: The incidence of rare-infiltrative type muscle pathology may be a predictive marker of DM with malignancy.

1. Introduction

The characteristic pathological muscular findings of polymyositis (PM) and dermatomyositis (DM) were shown early to reflect their different pathogeneses [1–4]. Cell-mediated immunity may occur in PM patients; CD8+ lymphocytes are aggregated around individual muscle fibers via MHC Class I-mediated antigen presentation on the muscle fiber plasma membrane, and endomysial lymphocyte infiltration is also characteristic [4]. On the other hand, DM is characterized by humoral immunity-mediated deposition of immune complexes, membrane attack complex (MAC) in the muscle bundle vascular wall, especially the infiltration of CD4+ lymphocytes around the perimysial blood vessels, and perifascicular atrophy [4,5]. In 1982, we encountered a DM patient with gastric cancer who showed some muscle fiber degeneration, a high creatine kinase (CK) level, and a rare infiltration of inflammatory cells without the typical perivascular cell infiltration and perifascicular atrophy usually observed in DM patients. Since then, we have paid special attention to such atypical findings in biopsied muscle to determine whether they might be a predictive marker of DM with malignancy. The numbers of muscle biopsies of PM and DM patients expanded to 215 over 40 years, and here we report the results of a statistical analysis of these muscle pathological findings.

2. Patients and methods

2.1. Patients

The study was approved by the Ethics Committee of the Kumamoto University Hospital. We retrospectively analyzed serial 215 PM/DM patients (PM: 161, DM: 54), who met either the "definite" or "probable" category of Bohan/Peter's criteria [6] and moreover underwent muscle biopsy between 1970 and 2009. Patients showing rimmed vacuoles on pathological examination (possible inclusion body myositis), and others showing other characteristic clinical features [7,8] were excluded. Patients with myopathy associated with anti-signal recognition particle (SRP) antibodies [9–11], exposure to statins [12,13], and paraneoplastic necrotizing myopathy [14,15] were also excluded.

In most of the patients with PM or DM, the muscle biopsy was performed before the start of steroid therapy; the one exception was a single patient complicated with rheumatoid arthritis who was taking 5 mg prednisolone.

* Corresponding author at: Department of Neurology, Faculty of Life Sciences, Kumamoto University, 1-1-1 Honjo, Kumamoto 860-0811, Japan.
Tel.: +81 96 373 5890; fax: +81 96 373 5895.
E-mail address: uchino@jonan-hospital.or.jp (M. Uchino).
[1] These authors contributed equally to this work.

0303-8467/$ – see front matter © 2012 Elsevier B.V. All rights reserved.
http://dx.doi.org/10.1016/j.clineuro.2012.07.019

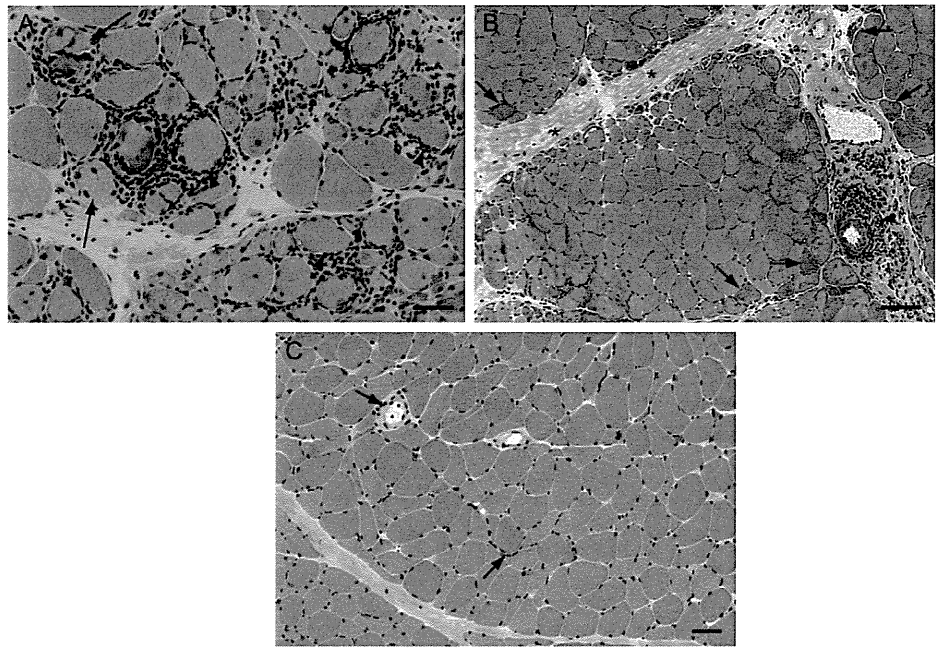

Fig. 1. Hematoxylin and eosin-stained muscle biopsy sections from biceps brachii showing 3 types of muscle pathology in PM (A) and DM (B and C) patients. (A) Endomysial infiltration-type, characterized by muscle fiber necrosis/regeneration (arrows), and lymphocyte infiltration around non-necrotic muscle fibers (arrowheads) in the muscle bundle of a 59-year-old female PM patient without malignancy. (B) Perivascular infiltration-type characterized by muscle fiber necrosis/regeneration (arrows), lymphocyte infiltration around perimysial blood vessels (arrowheads), and associated with perifascicular atrophy (asterisks) in a 74-year-old male DM patient without malignancy. (C) Rare-infiltrative-type without marked lymphocyte infiltration (i.e., only scarce distribution of lymphocytes was present; arrows) in a 61-year-old female DM patient with malignancy. Scale bars = 50 μm in A, 100 μm in B and C.

2.2. Histochemical analysis

Frozen sections of biopsies from the biceps or deltoid muscles of the arm, or quadriceps muscles of the thigh showing marked muscular weakness were stained with hematoxylin and eosin (HE), modified Gomori trichrome, nicotinamide adenine dinucleotide (NADH)-tetrazolium reductase, periodic acid Schiff, adenosine triphosphatase (ATPase), and acid phosphatase. Three skilled neurologists evaluated the pathology of the sections and classified lesions into 3 types: (1) endomysial infiltration-type, characterized by muscle fiber necrosis/regeneration and lymphocyte infiltration around non-necrotic muscle fibers in the muscle bundle; (2) perivascular infiltration-type, characterized by muscle fiber necrosis/regeneration, lymphocyte infiltration around perimysial blood vessels, and associated with perifascicular atrophy; and (3) rare-infiltrative-type [16], characterized by only sparse lymphocyte infiltration, some muscle fiber degeneration without perivascular cell infiltration, and perifascicular atrophy (Fig. 1).

In 19 representative DM patients, 7 with malignancies (3 perivascular infiltration type, and 4 rare-infiltrative type), and 12 without malignancies (4 perivascular infiltration-type, 3 endomysial infiltration-type, and 5 rare-infiltrative type), we conducted immunohistochemical staining with the following antibodies: anti-MHC Class I (cat. #M0736; Dako, Glostrup, Denmark), mouse anti-MHC Class II (cat. #M0746; Dako), mouse anti-CD4 (cat. #346320; Becton Dickinson, Franklin Lakes, NJ, USA), mouse anti-CD8 (cat. #346310, Becton Dickinson), mouse anti-CD19 (cat. #347540, Becton Dickinson), mouse anti-CD56 (cat. #PN 6603067; Beckman Coulter, Brea, CA, USA), mouse anti-CD45RO (cat. #M0742; Dako), and mouse anti-IgG/MAC (cat. #ab66768; Abcam, Cambridge, MA, USA). Similar staining was performed in 20 representative PM patients, 6 with malignancies (2 perivascular infiltration-type, 3 endomysial infiltration-type, and 1 rare-infiltrative type), 14 without malignancies (2 perivascular infiltration-type, 3 endomysial infiltration-type, and 9 rare-infiltrative type) and 3 normal control subjects. Immunolabeled proteins were visualized using the avidin–biotin–peroxidase complex (ABC) method with a Vectastain Elite ABC kit (Vector Laboratories, Burlingame, CA, USA).

2.3. Statistics

The statistical analyses of differences among results were conducted using Pearson's Chi-square test with Fisher's exact test (JMP version 7.0; SAS Institute, Cary, NC, USA).

3. Results

The mean (±SD) age of all PM patients ($n = 161$) on the initial consultation was 55.8 ± 15.4 years (range: 17–82 years) and that of PM patients with malignancies ($n = 9$) was 68.6 ± 9.6 (range: 56–82 years). The mean age of all DM patients ($n = 54$) was 50.5 ± 18.5 years (range: 15–88 years), and that of DM patients with malignancies ($n = 11$) was 59.5 ± 9.5 years (range: 41–70 years). In PM patients with malignancies, only 1 of 9 was already diagnosed with malignancy at the time of biopsy, while of the DM patients with malignancies, 3 of 11 patients were already diagnosed with malignancies at the time of biopsy. Malignancies were detected only in patients over 40 years of age. The clinical features of DM such as proximal dominant muscle weakness and skin rash (a heliotrope rash, Gottron's papules, paronychial erythema, and erythema squamosum of the stretching side of elbow and knee) were common without reference to malignancy.

The pathology findings of muscle biopsies are summarized in Table 1. Among the DM patients, the incidence of rare-infiltrative lesions in those with malignant tumors (45%) was significantly

Table 1
Pathology findings of muscle biopsies from 215 patients with polymyositis or dermatomyositis.

Disease status	Endomysial infiltration-type	Perivascular infiltration-type	Rare-infiltrative type
Polymyositis (n = 161)	97 (60%)	18 (11%)	46 (29%)
Without malignancy (n = 152)	91 (60%)	16 (11%)	45 (30%)
With malignancy (n = 9)	6 (67%)	2 (22%)	1 (11%)
Dermatomyositis (n = 54)	6 (11%)	37 (69%)	11 (20%)
Without malignancy (n = 43)	6 (14%)	31 (72%)	6 (14%)
With malignancy (n = 11)	0	6 (55%)	5 (45%)*

* p = 0.0345 dermatomyositis without malignancy vs with malignancy; Fisher's exact test.

higher than in those without such tumors (14%) (Pearson's Chi-square test: p = 0.0206; Fisher's exact test: p = 0.0345). There was no difference between the PM patients with and without malignancies.

To further evaluate the pathology of muscle biopsies, we selected typical patients from each group and conducted immunohistochemistry with anti-MAC, anti-MHC Class I/II, and anti-CD45RO antibodies. In normal controls (n = 3), MAC deposition was not observed in muscle bundle microvascular walls, the surface membranes of muscle fibers were not stained with anti-MHC Class I antibody, and there were no CD45RO-positive lymphocytes. In PM patients with endomysial infiltration with (n = 3) or without malignancies (n = 3), MAC deposition was not observed in muscle bundle microvascular walls, but necrotic muscle fibers, and perimysial vascular walls were faintly or clearly stained. The surface membranes of muscle fibers were strongly to faintly stained with anti-MHC Class I antibody in these patients. In PM patients with perivascular infiltration with (n = 2) or without malignancies (n = 2), MAC deposition was observed in muscle bundle microvascular walls, degenerative and necrotic muscle fibers, and perimysial vascular walls. The surface membranes of muscle fibers were strongly to faintly stained with anti-MHC Class I antibody in these patients. In the rare-infiltrative type PM patients with (n = 1) or without malignant tumors (n = 9), MAC deposition was not observed in muscle bundle microvascular walls. The surface membranes of muscle fibers were strongly to faintly stained with anti-MHC Class I antibody in more than 90% of the muscle fibers in these patients. In representative DM patients with perivascular infiltration with (n = 3) or without malignancies (n = 4), MAC deposition was observed in muscle bundle microvascular walls, degenerative and necrotic muscle fibers, and perimysial vascular walls (Fig. 2A). With anti-MHC Class I antibody, the surface membranes of muscle fibers were clearly stained in more than 80% of the muscle fibers in these patients.

In the rare-infiltrative type DM patients with (n = 4) or without malignant tumors (n = 5), the anti-MHC Class I antibody strongly to faintly and patchily to uniformly stained 20% to more than 80% of muscle fiber surface membranes (Fig. 2B), and the perimysial vascular walls were lightly stained with MHC Class II antibody (data not shown). Anti-MAC antibody staining was not present in the muscle bundle microvascular walls of these patients (Fig. 2C). Anti-CD45RO antibody, a marker of activated T cells, showed a small number of infiltrating lymphocytes in the muscle bundle (Fig. 2D). CD4-positive

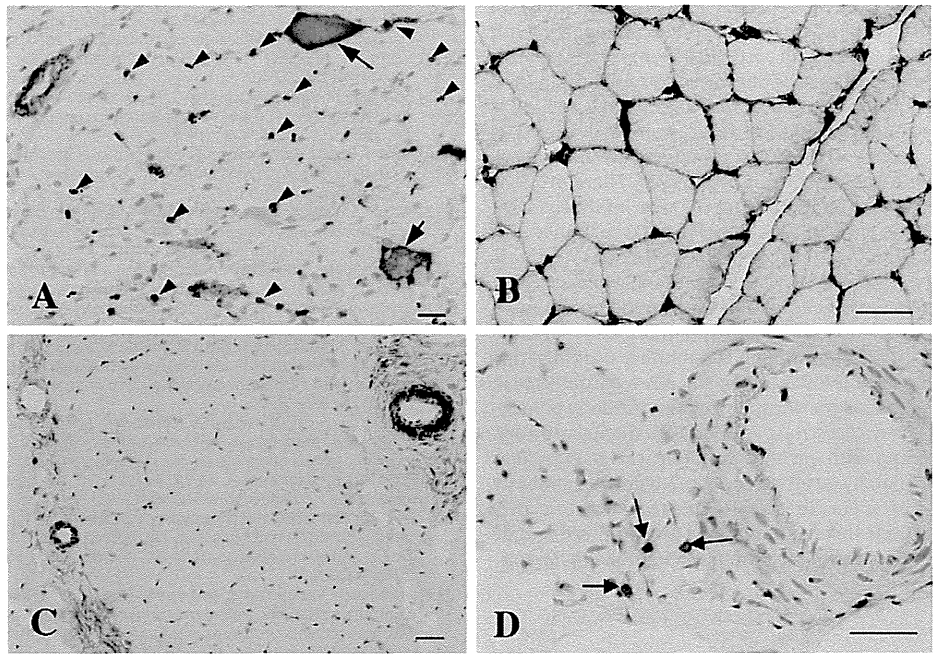

Fig. 2. Immunohistochemically stained biopsy sections from DM patients. (A) Anti-MAC antibody staining in a 50-year-old female representative of typical DM patients with perivascular infiltration showing MAC deposition in the muscle bundle microvascular walls (arrowheads), degenerative/necrotic muscle fibers (arrows), and perimysial vascular walls. (B) Anti-MHC Class I antibody staining in a 50-year-old female DM patient with breast cancer showing rare-infiltrative type muscle pathology typical of DM patients with malignant tumors; the muscle fiber surface membrane is uniformly stained. (C) Anti-MAC staining in a section from the same patient shown in (B) showing no staining in the muscle bundle microvascular wall. (D) Anti-CD45RO antibody (marker of activated T cells) staining in the same patient shown in (B and C). A small number of infiltrating lymphocytes in the muscle bundle show a positive reaction (arrows). Scale bars = 50 μm.

lymphocytes were very rare, and CD8-positive lymphocytes were not detected.

4. Discussion

Characteristic pathological findings of PM and DM reflect their different pathogeneses. Cell-mediated immunity may occur in PM patients. When the host is infected with an unknown virus or pathogen, CD8+ lymphocytes may be aggregated around individual muscle fibers via MHC Class I-mediated antigen presentation on the muscle fiber plasma membrane, affecting these fibers via perforin and granzyme secretion, and leading to necrosis or apoptosis, although no trigger has been clarified [4,17,18]. On the other hand, DM is characterized by humoral immunity-mediated deposition of immune complexes and MAC in the muscle bundle vascular wall, especially the infiltration of CD4+ lymphocytes around the perimysial blood vessels, and perifascicular atrophy [4,5]. Thus, a decrease in the vascular bed related to microvascular injury of the muscle bundle may result in the ischemia of muscle fibers around the muscle bundle with insufficient blood flow distant from the major artery, leading to degenerative necrosis.

We observed 54 typical DM patients over the course of 40 years, and the majority (69%) showed perivascular cell infiltration with perifascicular atrophy. However, a small number of DM patients (20%) showed a rare cell infiltration without perifascicular atrophy. Of this latter group, 5 out of 11 (45%) had malignancies. Thus, in DM patients with malignancies, the proportion of rare-infiltrative type lesions was significantly higher than in those without malignancies (14%). Furthermore, there was no MAC deposition in the muscle bundle microvascular wall and muscle fibers in any of the rare-infiltrative type DM patients with malignancies, suggesting a non-complement-mediated immune response. These immunohistological findings appear to be quite different from those of paraneoplastic necrotizing myopathy [15], and myopathy with antibodies to the signal recognition particle [9], where MAC deposition was observed in necrotic myofibers or endomysial capillaries. Of the myositis-specific autoantibodies, anti-155/140 antibody is well known to be a specific marker for cancer-associated DM [19–22]. However, specific characteristic findings are not always clear for the muscle pathology of this group [23]. Therefore, it is necessary to investigate the relationship of the rare-infiltrative type lesion and anti-155/140 antibody positive DM. In DM patients with malignancies and rare-infiltrative type lesions, MHC Class I expression was observed on the muscle fiber membrane. However, it is well known that MHC Class I expression is observed on the muscle fiber membrane of all inflammatory myopathies, and that there is no disease specificity [24]. Although the number of infiltrating cells was very small, some CD45RO-positive T cells were detected in these DM patients with malignancies, suggesting antibody production by memory T cells with a strong antibody-producing capacity. On preliminary staining with anti-IgG antibody, the muscle fiber membrane showed a patchy positive reaction, suggesting antibody binding to muscle fibers. Further studies are necessary to clarify the mechanism of muscle involvement in the rare-infiltrative type DM patients with malignancies including the relationship of anti-155/140 antibody.

5. Conclusion

Among DM patients, the incidence of rare-infiltrative type muscle pathology in those with malignancy was significantly higher than in those without such tumors, indicating that this pathology may be a predictive marker of DM with malignancy.

Conflict of interest

None.

Acknowledgements

We thank Drs. Y. Ando, S. Imamura, M. Nakajima, S. Mita, E. Uyama, and all members of the Department of Neurology, Kumamoto University for their support throughout the project.

References

[1] Behan WM, Barkas T, Behan PO. Detection of immune complexes in polymyositis. Acta Neurologica Scandinavica 1982;65:320–34.
[2] Arahata K, Engel AG. Monoclonal antibody analysis of mononuclear cells in myopathies. I. Quantitation of subsets according to diagnosis and sites of accumulation and demonstration and counts of muscle fibers invaded by T cells. Annals of Neurology 1984;16:193–208.
[3] Dalakas MC. Immunopathogenesis of inflammatory myopathies. Annals of Neurology 1995;37(Suppl. 1):S74–86.
[4] Dalakas MC, Hohlfeld R. Polymyositis and dermatomyositis. Lancet 2003;362:971–82.
[5] Emslie-Smith AM, Engel AG. Microvascular changes in early and advanced dermatomyositis: a quantitative study. Annals of Neurology 1990;27:343–56.
[6] Bohan A, Peter JB, Bowman RL, Pearson CM. Computer-assisted analysis of 153 patients with polymyositis and dermatomyositis. Medicine 1977;56:255–86.
[7] Griggs RC, Askanas V, DiMauro S, Engel A, Karpati G, Mendell JR, et al. Inclusion body myositis and myopathies. Annals of Neurology 1995;38:705–13.
[8] Karpati G, O'Ferrall EK. Sporadic inclusion body myositis: pathogenic considerations. Annals of Neurology 2009;65:7–11.
[9] Miller T, Al-Lozi MT, Lopate G, Pestronk A. Myopathy with antibodies to the signal recognition particle: clinical and pathological features. Journal of Neurology, Neurosurgery and Psychiatry 2002;73:420–8.
[10] Dimitri D, Andre C, Roucoules J, Hosseini H, Humbel RL, Authier FJ. Myopathy associated with anti-signal recognition peptide antibodies: clinical heterogeneity contrasts with stereotyped histopathology. Muscle and Nerve 2007;35:389–95.
[11] Suzuki S, Satoh T, Sato S, Otomo M, Hirayama Y, Sato H, et al. Clinical utility of anti-signal recognition particle antibody in the differential diagnosis of myopathies. Rheumatology 2008;47:1539–42.
[12] Kogan AD, Orenstein S. Lovastatin-induced acute rhabdomyolysis. Postgraduate Medical Journal 1990;66:294–6.
[13] Mohaupt MG, Karas RH, Babiychuk EB, Sanchez-Freire V, Monastyrskaya K, Iyer L, et al. Association between statin-associated myopathy and skeletal muscle damage. Canadian Medical Association Journal 2009;181:E11–8.
[14] Levin MI, Mozaffar T, Al-Lozi MT, Pestronk A. Paraneoplastic necrotizing myopathy: clinical and pathological features. Neurology 1998;50:764–7.
[15] Sampson JB, Smith SM, Smith AG, Singleton JR, Chin S, Pestronk A, et al. Paraneoplastic myopathy: response to intravenous immunoglobulin. Neuromuscular Disorders 2007;17:404–8.
[16] Imai T, Hirayama K, Osumi E. Muscle histopathology and responsiveness to steroid therapy in polymyositis and dermatomyositis. Rinsho Shinkeigaku Clinical Neurology 1995;35:243–6.
[17] Orimo S, Koga R, Goto K, Nakamura K, Arai M, Tamaki M, et al. Immunohistochemical analysis of perforin and granzyme A in inflammatory myopathies. Neuromuscular Disorders 1994;4:219–26.
[18] Cherin P, Herson S, Crevon MC, Hauw JJ, Cervera P, Galanaud P, et al. Mechanisms of lysis by activated cytotoxic cells expressing perforin and granzyme-B genes and the protein TIA-1 in muscle biopsies of myositis. Journal of Rheumatology 1996;23:1135–42.
[19] Kaji K, Fujimoto M, Hasegawa M, Kondo M, Saito Y, Komura K, et al. Identification of a novel autoantibody reactive with 155 and 140 kDa nuclear proteins in patients with dermatomyositis: an association with malignancy. Rheumatology 2007;46:25–8.
[20] Chinoy H, Fertig N, Oddis CV, Ollier WE, Cooper RG. The diagnostic utility of myositis autoantibody testing for predicting the risk of cancer-associated myositis. Annals of the Rheumatic Diseases 2007;66:1345–9.
[21] Fujikawa K, Kawakami A, Kaji K, Fujimoto M, Kawashiri S, Iwamoto N, et al. Association of distinct clinical subsets with myositis-specific autoantibodies towards anti-155/140-kDa polypeptides, anti-140-kDa polypeptides, and anti-aminoacyl tRNA synthetases in Japanese patients with dermatomyositis: a single-centre, cross-sectional study. Scandinavian Journal of Rheumatology 2009;38:263–7.
[22] Hamaguchi Y, Kuwana M, Hoshino K, Hasegawa M, Kaji K, Matsushita T, et al. Clinical correlations with dermatomyositis-specific autoantibodies in adult Japanese patients with dermatomyositis: a multicenter cross-sectional study. Archives of Dermatology 2011;147:391–8.
[23] Ohashi M, Shu E, Tokuzumi M, Fujioka K, Ishizuka T, Hara A, et al. Anti-p155/140 antibody-positive dermatomyositis with metastasis originating from an unknown site. Acta Dermato: Venereologica 2011;91:84–5.
[24] Jain A, Sharma MC, Sarkar C, Bhatia R, Singh S, Handa R. Major histocompatibility complex class I and II detection as a diagnostic tool in idiopathic inflammatory myopathies. Archives of Pathology and Laboratory Medicine 2007;131:1070–6.

Original Paper

European Neurology

Eur Neurol 2012;68:117–121
DOI: 10.1159/000338474

Received: January 12, 2012
Accepted: March 23, 2012
Published online: July 11, 2012

Long-Term Outcome of Polymyositis Treated with High Single-Dose Alternate-Day Prednisolone Therapy

Makoto Uchino[a, b] Satoshi Yamashita[a] Katsuhisa Uchino[a, b] Akio Hara[a] Tatsuya Koide[a, b] Tomohiro Suga[a] Tomoo Hirahara[a] En Kimura[a] Taro Yamashita[a] Akihiko Ueda[a] Ryoichi Kurisaki[a] Junko Suzuki[a] Shoji Honda[a] Yasushi Maeda[a] Teruyuki Hirano[a]

[a]Department of Neurology, Faculty of Life Sciences, Kumamoto University, and [b]Department of Neurology, Jonan Hospital, Mubanchi Jonanmachi, Kumamoto, Japan

Key Words
Polymyositis · High single-dose alternate-day prednisolone therapy · Daily-dose prednisolone therapy

Abstract
Background: We previously reported no difference in the efficacies of high-dose alternate-day (ADT) and daily-dose (DDT) prednisolone therapies in myositis patients, but that the incidence of side effects was lower in the former. The aim of the present study was to compare the long-term outcomes of both treatments in polymyositis patients. ***Methods:*** We compared clinical courses, efficacies, adverse reactions, and outcomes of 115 consecutive, biopsy-proven polymyositis patients treated between 1970 and 2008 with ADT (32 patients) or DDT (83 patients). ***Results:*** Mean onset ages, disease severity, incidences of malignancy, and response rates did not differ between the ADT and DDT groups. Adverse reactions (incidence of diabetes) were significantly higher in the DDT group. In this group, the incidences of hyperlipidemia, infection, hypertension, and psychiatric symptoms were also slightly higher, but not significantly so. The 20-year survival rate of the ADT group (68%) was significantly higher ($p = 0.0112$) than that of the DDT group (37%). ***Conclusion:*** ADT might be useful as an initial treatment option for polymyositis.

Introduction

In the 1970s, polymyositis (PM)/dermatomyositis (DM) was mainly treated with daily-dose prednisolone therapy (DDT). However, the side effects of steroids (e.g. moon face, central obesity, diabetes, osteoporosis with morbid fracture, hypertension, and infection-prone features) were frequently observed and considered to be unavoidable. In 1963, high-dose alternate-day prednisolone therapy (ADT) was proposed to reduce the side effects of prednisolone (PSL) in the treatment of various diseases involving immune disorders, such as bronchial asthma [1]. We have employed ADT in patients with PM/DM since 1971. Daily-dose PSL at 50 mg/day was switched to

M.U., S.Y., K.U., A.H., and T.K. contributed equally to this work.

KARGER

Fax +41 61 306 12 34
E-Mail karger@karger.ch
www.karger.com

0014–3022/12/0682–0117$38.00/0

Accessible online at:
www.karger.com/ene

Makoto Uchino
Department of Neurology, Faculty of Life Sciences
Kumamoto University
1-1-1 Honjo, Kumamoto 860-0811 (Japan)
Tel. +81 96 373 5890, E-Mail uchino@jonan-hospital.or.jp

ADT at 100 mg/day; in addition to morning administration, a diet for diabetics, salt restriction to <6 g/day, and treatment with potassium/active vitamin D preparations were introduced. We previously reported that there was no difference in the response rates between 30 PM/DM patients receiving ADT and 17 receiving DDT, but that the incidence of side effects was markedly lower in the former [2]. We have now evaluated the long-term outcomes of ADT and DDT so as to design a future prospective study. We compared response rates, adverse reactions, and long-term prognoses of 115 patients receiving either ADT or DDT as initial treatment for PM.

Patients and Methods

Patients

We clinically analyzed 235 patients with inflammatory myopathy who consulted our department between 1970 and 2009. Of 161 patients who were diagnosed histologically [3] as having PM, 149 were treated with ADT (35 patients) or DDT (114 patients). In the present study, we analyzed 115 of the PM patients who were followed more than 10 years or until death: 32 ADT patients and 83 DDT patients. Patients showing rimmed vacuoles and intracellular amyloid deposits on pathological examination (possible inclusion body myositis), and others showing characteristic clinical features, such as finger flexor, wrist flexor, and quadriceps muscle weakness [4, 5], were excluded. Patients with myopathy associated with anti-signal recognition particle antibodies that have usually shown active necrosis and little or no inflammation [6–8], statin-induced myopathy that shows features suggestive of mitochondrial dysfunction [9, 10], and paraneoplastic necrotizing myopathy that exhibits numerous necrotic fibers but little inflammation [11, 12] were also excluded. We also excluded patients who did not show electromyography findings compatible with inflammatory myopathy; that is increased insertional activity, fibrillation potentials, and positive sharp waves, in addition to polyphasic motor unit potentials of low amplitude and short duration.

DDT was administered to all inpatients from 1970 through 1971. ADT was administered to almost all inpatients from 1972 through 1983 for a trial of about 10 years to confirm if it reduced the side effects of steroids. Following the completion of these scheduled periods, most of the inpatients underwent DDT from 1984 through 2008. Those patients initially receiving one or the other therapy were continued on that therapy when the convention was changed.

ADT consisted initially of a single 2-mg/kg dose of PSL in the morning every other day; after monitoring normalized serum creatine kinase (CK) and improvements in clinical symptoms, the dosage was lowered by 10 mg every 3–4 weeks, until it reached the 10–30 mg range, where it was maintained for several years. DDT consisted of a single morning dose of 1 mg/kg PSL; after normalization of serum CK and improvements in clinical symptoms, the dosage was lowered by 5 mg every 3–4 weeks, until it reached the 5–15 mg range, where it was maintained for several years. For both groups, a diabetic diet was prescribed with salt limited to <6 g/day, and potassium/active vitamin D and anti-ulcer agents were administered.

Clinical Parameters

We compared the following parameters between the ADT and DDT groups: age at onset or initial consultation, gender, presence or absence of malignancy, presence or absence of other collagen diseases including Sjögren's syndrome, grading of disability [13] before and after treatment and during follow-up periods, presence or absence of interstitial pneumonia or cardiomyopathy, increase in CK level (>1,000 IU/L), anti-Jo-1 antibody, presence or absence of methylprednisolone pulse therapy and other immunosuppressants, and incidences of major side effects (hypertension, diabetes, osteoporosis with morbid fracture, infection, hyperlipidemia, psychiatric symptoms, and gastric ulcer).

Clinical Outcome

As a measure of outcome, treatment response was evaluated based on pretreatment manual muscle testing (MMT) results and disability scores in each patient. Muscle strength was measured weekly in the case of inpatients and monthly in the case of outpatients by MMT using the Medical Research Council method on the following muscles: trapezius, neck flexor, deltoid, pectoralis major, infraspinatus, supraspinatus, biceps, triceps, wrist extensor, wrist flexor, iliopsoas, gluteus maximus, quadriceps, hamstring, adductor of thigh, abductor of thigh, gastrocnemius + soleus, and tibialis anterior. Values were totaled and compared with pretreatment figures as described previously [2]. The grading of disability [13] included six grades: (1) no abnormality on examination; (2) no abnormality on examination, but patient-reported easy fatigability and decreased exercise tolerance (e.g. running and climbing stairs); (3) minimal degree of weakness or atrophy in one or more muscle groups without functional impairment (limitation of actual daily life); (4) waddling gait, unable to run but able to climb stairs without needing arm support; (5) marked waddling gait, unable to climb stairs or rise from a standard high chair without arm support, and (6) unable to walk without assistance. In addition to attendant physicians, Prof. Uchino evaluated all patients.

Patients with normal MMT findings and improved disability scores without PSL therapy were classified as 'cured'. Those in whom maintenance therapy with PSL was continued despite a one-grade or higher amelioration of the MMT results for the upper and lower limb muscles and improvement in disability scores were regarded as 'improved'. Those without marked improvement in MMT findings and disability scores, despite a normalized CK level, were designated as 'unchanged'. Those who died during the treatment course were classified as 'death cases'. The first and second groups were evaluated as responders, and the third and fourth groups as non-responders. Survival rates were analyzed using the Kaplan-Meier method. Statistical differences were determined by Pearson's χ^2, and log-rank tests using JMP (version 7.0) statistical software. Differences with $p < 0.05$ were considered significant. Values are reported as means ± SD.

Results

The demographic and clinical characteristics of the 115 PM patients treated with ADT or DDT are summarized in table 1. The mean (±SD) age of the PM patients on the initial consultation was 55.5 ± 15.1 years (range 17–82) and

that of the PM patients with malignancies (n = 8) was 68.9 ± 10.2 years (range 56–82). Malignancies were detected only in patients over 50 years of age. There were no significant differences in mean onset age, gender, or incidence of malignancies between the two groups, or in the response rates (complete and partial responses) between the ADT (87.5%) and DDT (80.7%) groups. Although the recruitment and patient allocation was not necessarily randomized, there was no significant difference in disease severity using the grading of disability between the ADT and DDT groups: 4.56 ± 0.98 in the ADT versus 4.31 ± 0.76 in the DDT (p = 0.1520). The mean fasting blood sugar level of the ADT group before treatment was 86.1 ± 13.0 mg/dl (n = 32) and that of DDT group was 85.3 ± 12.4 mg/dl (n = 85) (normal range 70–110 mg/dl). There was no significant difference between the two groups (p = 0.8681).

PM patients treated with ADT were followed for 222.7 ± 124.9 months (range 13–458), while the DDT group was followed for 151.2 ± 87.9 months (range 3–414). The incidence of diabetes (ADT 6.3%, DDT 36.1%; p = 0.0384) was significantly higher in the DDT group. The incidences of hyperlipidemia (ADT 3.1%, DDT 14.5%; p = 0.0854) and psychiatric symptoms (ADT 0%, DDT 8.4%; p = 0.0900) were also slightly higher in the DDT group, but not significantly so.

When the patients with pulse therapy are excluded from the DDT group, the incidence of hyperlipidemia (ADT 3.1%, DDT 18.2%; p = 0.0393) was significantly higher in the DDT group. The incidences of diabetes (ADT 6.3%, DDT 21.2%; p = 0.0602), hypertension (ADT 3.1%, DDT 15.2%; p = 0.0770), and psychiatric symptoms (ADT 0%, DDT 10.6%; p = 0.0559) were also slightly higher in the DDT group, but not significantly so. The main causes of death in both the DDT and ADT groups were infections, such as pneumonia, cytomegalovirus infection, liver abscess, peritonitis, and sepsis, followed by newly occurring cancer. Death by infection occurred in 4 of 32 patients treated with ADT and in 14 of 83 patients in the DDT group (p = 0.5635). Death by cancer also occurred in 4 of 32 patients in the ADT group and in 5 of 83 patients in the DDT group (p = 0.2466). In patients followed more than 20 years, deaths due to coronary heart disease, cerebral infarction, and renal failure due to diabetic nephropathy were observed in 8 of 49 patients in the DDT group; however, none of these were seen in the 25 ADT patients. Respiratory disorders related to the progress of interstitial pneumonia were observed in both the DDT and ADT groups. The main causes of death were similar if the patients with pulse therapy or other immunosuppressants therapy were excluded from the DDT group.

Table 1. Baseline demographic and clinical characteristics of 115 biopsy-proven patients with PM treated by ADT

Characteristics	ADT group (n = 32; 27.8%)	DDT group (n = 83; 72.2%)	p value
Onset age, years	49.9 ± 14.5	55.3 ± 14.9	0.0818
Age at diagnosis, years	52.0 ± 14.8	56.8 ± 15.0	0.1199
Number of females	25 (78.1%)	57 (68.7%)	0.3154
Malignancy	2 (6.3%)	6 (7.2%)	0.8533
Other collagen disease	6 (18.8%)	19 (22.9%)	0.6294
Grading of disability			
Before treatment	4.56 ± 0.98	4.31 ± 0.76	0.1520
After treatment	2.84 ± 1.30	2.66 ± 1.21	0.4817
Follow-up period, months	222.7 ± 124.9	151.2 ± 87.9	0.0009*
Interstitial pneumonia	5 (15.6%)	12 (14.5%)	0.8744
Cardiomyopathy	3 (9.4%)	6 (7.2%)	0.7010
CK level >1,000 IU/L	13 (40.6%)	51 (61.4%)	0.044*
Jo-1-positive	4 (12.5%)	8 (9.6%)	0.6528
Pulse therapy	0	17 (20.5%)	0.0055*
Other immunosuppressant	2 (6.3%)	13 (15.7%)	0.1792
Major side effects			
Hypertension	1 (3.1%)	11 (13.3%)	0.1114
Diabetes mellitus	2 (6.3%)	30 (36.1%)	0.0384*
Hyperlipidemia	1 (3.1%)	12 (14.5%)	0.0854
Infection	3 (4.4%)	18 (21.7%)	0.1257
Osteoporosis with morbid fracture	2 (6.3%)	10 (12.0%)	0.3620
Psychiatric symptoms	0	7 (8.4%)	0.0900
Gastric ulcer	3 (9.4%)	2 (2.4%)	0.1007
Outcome			
Cure	3 (9.4%)	7 (8.4%)	0.8725
Improvement	25 (78.0%)	60 (72.3%)	0.5230
Unchanged · death	4 (12.5%)	15 (18.1%)	0.4709

Values are expressed as means ± SD, unless indicated otherwise.
* $p < 0.05$ by Pearson's χ^2 test.

When all patients were considered, there was no difference in the 10-year survival rates between the ADT and DDT groups (fig. 1a), but both the 15-year (data not shown; ADT 67%, DDT 47%; p = 0.0780) and 20-year (ADT 68%, DDT 37%; p = 0.0112) survival rates of the ADT group were significantly higher than those of the DDT group (fig. 1b), and this difference increased over the 20 years following onset.

Of the patients receiving DDT, 17 also received 1–3 courses of pulse therapy with methylprednisolone. Immunosuppressants other than PSL were used in 2 patients in the ADT group (tacrolimus hydrate in 1 and azathioprine in 1) and in 13 patients of the DDT group (tacrolimus hydrate in 4, azathioprine in 5, cyclosporine in 2, methotrexate in 2, IVIg in 2, and endoxan in 1).

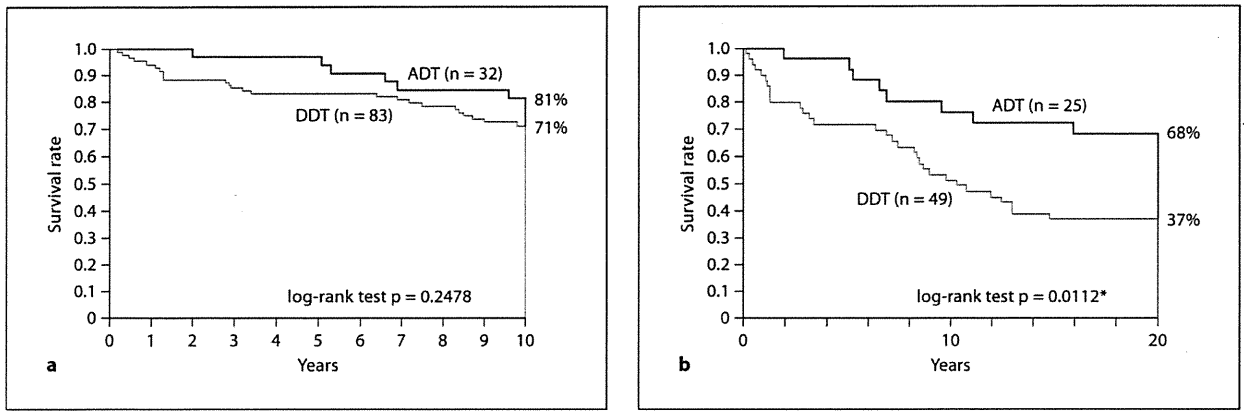

Fig. 1. Kaplan-Meier plots showing survival rates in PM patients treated with ADT or DDT: **a** 10-year survival rates of PM patients treated with ADT and DD, and **b** 20-year survival rates of PM patients treated with ADT and DDT. log-rank test indicates a significantly longer survival time in the ADT group after 20 years.

Discussion

Since ADT was first introduced to treat immune disorders, it has also been used in patients with various immunogenic neuromuscular disorders [14–17]. During the more than 20 years since we began using ADT therapy, the number of PM/DM patients treated with ADT or DDT increased more than three times. The number of PM patients in whom ADT was introduced as the initial treatment was small; the greater portion of these subjects consisted of patients who were treated between 1972 and 1983, when ADT was undertaken in almost all inpatients. After 1983, we switched back to DDT due to the completion of a scheduled 10-year analysis period. However, we statistically reconfirmed that there was no difference in the response rates of the two groups, and that the incidence of major side effects was significantly lower in the ADT group. Furthermore, in the ADT group, the survival rates (both 15- and 20-year) were significantly higher than in the DDT group. This was possibly because the incidence of adverse reactions, especially those influencing prognosis (diabetes, hyperlipidemia, infection, and its exacerbations) were lower in the ADT group. Even when the patients with pulse therapy were excluded from the DDT group, the incidence of major side effects, such as hyperlipidemia, diabetes mellitus, psychiatric symptoms, hypertension, and infection were still higher in the DDT group than in the ADT group.

Recently, many studies reported on the etiology or pathogenesis of PM/DM, increasing treatment options with the widespread use of various immunosuppressive agents [18, 19]. Furthermore, pathogenesis-based molecular targeting agents are being developed and applied in clinical practice [20–24]. The major causes of death in the PM patients were infection, followed by newly occurring malignancies. Although there is the possibility that other immunosuppressants induced such conditions, none of the DDT patients who died from infection or malignancy were treated with other immunosuppressants. So, the influence of other immunosuppressants was neglected. The coronary heart disease, cerebral infarction, and diabetic nephropathy observed in the DDT group are likely due to the high frequency of diabetes mellitus, hyperlipidemia, and hypertension, and may be related to the low survival rate of this group.

As previously described, 1–3 courses of pulse therapy with methylprednisolone were performed in 17 of the PM patients receiving DDT. Immunosuppressants other than PSL were used in 2 patients in the ADT group and in 13 patients of the DDT group. There was no statistical difference in the use of other immunosuppressants between the ADT group and DDT group. Although there was a significant difference in the use of methylprednisolone pulse therapy between the ADT group and DDT group, survival rates were not different between the pulse therapy group (9/17: 53%) and the no pulse therapy group (60/98: 61%) ($p = 0.5199$). Considering the lack of significant difference in response rates between the ADT and DDT groups, and the differences in the 15- and 20-year survival rates of the two groups, methylprednisolone

pulse therapy might not have contributed to the improvement in the long-term outcome of PM. Various studies have assessed the long-term outcome of PM/DM, however few have examined the long-term prognosis over more than 20 years [25–28]. Our study suggests that ADT may be useful as an initial treatment option for PM, and we intend to test this hypothesis in a prospective, comparative study of ADT and DDT using larger and equal numbers of subjects in each group.

Conclusions

ADT PSL therapy is a safe, effective treatment for PM. Its response rate was not significantly different from that of DDT, but adverse reactions (diabetes) were significantly lower and the incidences of hyperlipidemia, infection, and psychiatric symptoms were also slightly lower in the ADT group. Moreover, ADT led to a significantly higher survival rate in PM patients. Thus, ADT may be useful as an initial treatment option for PM.

Acknowledgements

We thank Drs. S. Imamura, M. Nakajima, S. Mita, E. Uyama, Y. Ando and all members of the Department of Neurology, Kumamoto University, for their support throughout the project.

Disclosure Statement

The authors have no conflicts of interest to disclose.

References

1 Harter JG, Reddy WJ, Thorn GW: Studies on an intermittent corticosteroid dosage regimen. N Engl J Med 1963;269:591–596.
2 Uchino M, Araki S, Yoshida O, Uekawa K, Nagata J: High single-dose alternate-day corticosteroid regimens in treatment of polymyositis. J Neurol 1985;232:175–178.
3 Dalakas MC, Hohlfeld R: Polymyositis and dermatomyositis. Lancet 2003;362:971–982.
4 Griggs RC, Askanas V, DiMauro S, Engel A, Karpati G, Mendell JR, Rowland LP: Inclusion body myositis and myopathies. Ann Neurol 1995;38:705–713.
5 Karpati G, O'Ferrall EK: Sporadic inclusion body myositis: Pathogenic considerations. Ann Neurol 2009;65:7–11.
6 Miller T, Al-Lozi MT, Lopate G, Pestronk A: Myopathy with antibodies to the signal recognition particle: clinical and pathological features. J Neurol Neurosurg Psychiatry 2002;73:420–428.
7 Dimitri D, Andre C, Roucoules J, Hosseini H, Humbel RL, Authier FJ: Myopathy associated with anti-signal recognition peptide antibodies: clinical heterogeneity contrasts with stereotyped histopathology. Muscle Nerve 2007;35:389–395.
8 Suzuki S, Satoh T, Sato S, Otomo M, Hirayama Y, Sato H, Kawai M, Ishihara T, Suzuki N, Kuwana M: Clinical utility of anti-signal recognition particle antibody in the differential diagnosis of myopathies. Rheumatology (Oxford) 2008;47:1539–1542.
9 Kogan AD, Orenstein S: Lovastatin-induced acute rhabdomyolysis. Postgrad Med J 1990; 66:294–296.
10 Mohaupt MG, Karas RH, Babiychuk EB, Sanchez-Freire V, Monastyrskaya K, Iyer L, Hoppeler H, Breil F, Draeger A: Association between statin-associated myopathy and skeletal muscle damage. CMAJ 2009; 181:E11–E18.
11 Levin MI, Mozaffar T, Al-Lozi MT, Pestronk A: Paraneoplastic necrotizing myopathy: clinical and pathological features. Neurology 1998;50:764–767.
12 Sampson JB, Smith SM, Smith AG, Singleton JR, Chin S, Pestronk A, Flanigan KM: Paraneoplastic myopathy: response to intravenous immunoglobulin. Neuromuscul Disord 2007;17:404–408.
13 Rose AL, Walton JN: Polymyositis: A survey of 89 cases with particular reference to treatment and prognosis. Brain 1966;89:747–768.
14 Axelrod L: Glucocorticoid Therapy. Medicine (Baltimore) 1976;55:39–65.
15 Cook JD, Trotter JL, Engel WK, Sciabbarrasi JS: The effects of single-dose alternate-day prednisone therapy on the immunological status of patients with neuromuscular diseases. Ann Neurol 1978;3:166–176.
16 Fauci AS, Dale DC, Balow JE: Glucocorticosteroid therapy: mechanisms of action and clinical considerations. Ann Intern Med 1976;84:304–315.
17 Streeten DH: Corticosteroid therapy. I. Pharmacological properties and principles of corticosteroid use. JAMA 1975;232:944–947.
18 Mastaglia FL, Zilko PJ: Inflammatory myopathies: How to treat the difficult cases. J Clin Neurosci 2003;10:99–101.
19 Dalakas MC, Illa I, Dambrosia JM, Soueidan SA, Stein DP, Otero C, Dinsmore ST, McCrosky S: A controlled trial of high-dose intravenous immune globulin infusions as treatment for dermatomyositis. N Engl J Med 1993;329:1993–2000.
20 Oddis CV, Sciurba FC, Elmagd KA, Starzl TE: Tacrolimus in refractory polymyositis with interstitial lung disease. Lancet 1999; 353:1762–1763.
21 Nadiminti U, Arbiser JL: Rapamycin (sirolimus) as a steroid-sparing agent in dermatomyositis. J Am Acad Dermatol 2005;52:17–19.
22 Levine TD: Rituximab in the treatment of dermatomyositis: an open-label pilot study. Arthritis Rheum 2005;52:601–607.
23 Majithia V, Harisdangkul V: Mycophenolate mofetil (CellCept): an alternative therapy for autoimmune inflammatory myopathy. Rheumatology (Oxford) 2005;44:386–389.
24 Labioche I, Liozon E, Weschler B, Loustaud-Ratti V, Soria P, Vidal E: Refractory polymyositis responding to infliximab: extended follow-up. Rheumatology (Oxford) 2004;43: 531–532.
25 Maugars YM, Berthelot JM, Abbas AA, Mussini JM, Nguyen JM, Prost AM: Long-term prognosis of 69 patients with dermatomyositis or polymyositis. Clin Exp Rheumatol 1996;14:263–274.
26 Benbassat J, Gefel D, Larholt K, Sukenik S, Morgenstern V, Zlotnick A: Prognostic factors in polymyositis/dermatomyositis. A computer-assisted analysis of ninety-two cases. Arthritis Rheum 1985;28:249–255.
27 Marie I, Hachulla E, Hatron PY, Hellot MF, Levesque H, Devulder B, Courtois H: Polymyositis and dermatomyositis: short-term and long-term outcome, and predictive factors of prognosis. J Rheumatol 2001;28: 2230–2237.
28 Airio A, Kautiainen H, Hakala M: Prognosis and mortality of polymyositis and dermatomyositis patients. Clin Rheumatol 2006;25: 234–239.